ABSTRACT

SADRI, AHMAD. The Effect of Special Wastes on Refuse Decomposition and Phosphorus Cycling in Laboratory-Scale Municipal Solid Waste Reactors. (Under the direction of Dr. Morton A. Barlaz).

In this research, the use of laboratory-scale tests to evaluate the effect of various non-hazardous wastes on refuse decomposition is demonstrated. Non-hazardous wastes are receiving increased interest from landfill owners especially with respect to bioreactor operation. These wastes could benefit bioreactors in that they represent sources of liquid, nutrients, and/or substrate. However, landfill operators should exercise caution in accepting these wastes, as some could have detrimental effects on refuse decomposition.

Three wastes were evaluated including (1) aerobically digested wastewater treatment plant biosolids which represent a nutrient source, (2) burnt sugar, which is a viscous glucose/lactic acid mixture from an agricultural process and represents a high carbon, acidic substrate, and (3) wastes from fabric softener and detergent production. As each waste had unique properties, testing protocols were adapted to address the specific concerns surrounding each material.

Biosolids were compatible with refuse decomposition but they did not increase maximum methane production rates and yields or reduce lag times to the onset of methane production. There is some evidence that biosolids increased phosphorus, but it was found to be not limiting. Burnt sugar experiments suggested that actively decomposing refuse has the potential to attenuate relatively high loading of a highly degradable and low pH substrate. Detergent experiments demonstrated significant inhibition of refuse decomposition at low waste additions.

THE EFFECT OF SPECIAL WASTES ON REFUSE DECOMPOSITION AND PHOSPHORUS CYCLING IN LABORATORY-SCALE MUNICIPAL SOLID WASTE REACTORS

by
AHMAD SADRI

A thesis submitted to the Graduate Faculty of
North Carolina State University
in partial fulfillment of the
requirements for the Degree of
Master of Science

ENVIRONMENTAL ENGINEERING

Raleigh, North Carolina

2007

APPROVED BY:

Dr. Detlef R. Knappe	Dr. Francis L. de los Reyes

Dr. Morton A. Barlaz
Chair of Advisory Committee

BIOGRAPHY

Ahmad Sadri was born in Esfahan, Iran, on July 6, 1983. He moved to Canada with his family and lived in Montreal, Quebec until 1990, when he moved to Greensboro, NC. He graduated from North Carolina State University in 2001 with a degree in Civil Engineering. Following the completion of his Master's, Ahmad will participate in a joint project with North Carolina State University and the University of Hawaii to explain hydrogen production at the Waimanolo Gulch Landfill.

ACKNOWLEDGEMENTS

Many thanks to all those who, without their expertise and dedication, this research could not have been possible:

Dr. Barlaz (who set me loose in the lab, was very patient and encouraging, who taught me all I know about solid waste and dramatically improved my writing… and he's sending me to HAWAII!!!)

Drs. Knappe and de los Reyes (their classes got me interested in environmental engineering in the first place)

Waste Management (who funded the project and supplied the wastes)

David Black (who performed solids composition and lactic acid analysis and provided training and good common sense laced with sarcasm)

Guillermo Ramirez, at NCSU Soil Science Department Analytical Services Laboratory (who performed analyses for NH_4, Fe, Ca, Mg, and Al)

Fang Xu (who analyzed VFA's and provided training)

Nathan McKittrick (who monitored detergent reactors, performed COD and gas analyses, and was always willing to come in at 3 am and help)

Jana Chaney (who performed BMP's, ATA's, and helped with shredding refuse)

Lauren Wellborn (who helped with collecting, filtering, and storing leachate samples)

Bryan Staley (who helped with monitoring the burnt sugar reactors, shredding refuse, and making municipal solid waste exciting)

Shannon Bartelt-Hunt (who provided gas production calculation spreadsheets)

Jason Tillotson (who performed Fe analysis and provided hours of entertainment with dry ice)

Hossain M. Azam (who helped with shredding refuse and provided engaging philosophical discussions)

Bilgen Yuncu (who performed a TOC analysis)

University of Georgia Complex Carbohydrate Research Center (sugar analysis)

University of Georgia Chemical Analysis Laboratory (CHN and ICP analyses)

And of course my friends and family, who have always supported me in all that I do.

TABLE OF CONTENTS

LIST OF TABLES

LIST OF FIGURES

1 BACKGROUND AND RESEARCH OBJECTIVES

There has been increased emphasis on the operation of landfills as bioreactors in the past decade (Benson et al. 2007; Reinhart et al., 2002). The potential advantages of bioreactor landfills have been described in detail previously and include (1) increased gas production and potential energy recovery, (2) increased settlement and waste density, (3) in-situ leachate treatment and (4) more rapid stabilization of the waste mass (Benson et al., 2007). As landfill owners become more interested in the operation of landfills as bioreactors, new strategies are being developed to optimize the implementation of this technology.

The need for sufficient moisture to thoroughly wet the buried waste has arisen as one limitation to the full-scale implementation of bioreactor landfills. While somewhat anecdotal, many landfill owners indicate that they do not receive sufficient infiltration from rain alone to wet the waste. This is consistent with a survey of practices at five North American bioreactor landfills that showed that many full-scale bioreactor landfills were not adding sufficient moisture to have a significant impact on overall waste moisture content (Benson et al., 2007). This is not surprising as 455 L/metric ton are required to adjust the moisture content from 20% to 45% where moisture content is expressed on a wet weight basis. For a landfill that receives 1000 metric tons/day, this equates to 455 m^3 of infiltration daily. At some landfills the need for water is addressed by recirculating leachate from the entire landfill into a relatively small section that is operated as a bioreactor. This strategy is only useful when a limited area is operated as a bioreactor and is not sustainable as bioreactor operations are scaled up. To this end, landfill owners have interest in the addition of liquids and wastes that have elevated moisture content.

In addition to the value of liquid wastes for their moisture, they also represent a mechanism for the diversion of high strength (i.e. BOD) liquids from publicly owned wastewater treatment plants (POTWs). In cases where POTWs are operating at capacity, the diversion of liquids to a landfill can forestall costly POTW upgrades or even allow for industrial development that would not otherwise be possible. This situation was observed at a landfill in the southeastern U.S. In addition, there is growing interest in the acceptance of non-hazardous industrial liquids in MSW landfills as a revenue source. Such wastes may contribute moisture, represent a carbonaceous substrate, or serve as a source of nutrients. In all cases, it is essential that any added wastes be compatible with the methanogenic conversion of cellulose, the principle biodegradable substrate in a landfill, to methane and carbon dioxide.

In this research, the use of laboratory-scale tests to evaluate the effect of various non-hazardous wastes on refuse decomposition is demonstrated. Three wastes were evaluated including aerobically digested wastewater treatment plant biosolids which represent a nutrient source, a viscous glucose/lactic acid mixture from an agricultural process which is a high carbon, acidic substrate, and wastes from the production of fabric softener and detergent. As each waste had unique properties, the testing protocol was adapted to address the specific concerns surrounding each material.

Research on the effect of biosolids on decomposition has been reviewed (Barlaz et al., 1990). Biosolids enhance refuse decomposition by providing nutrients and a seed of microorganisms, although their presence may result in excessive acid accumulation that requires intensive leachate neutralization. In this study, the objective was to evaluate the impact of biosolids addition on leachate P concentrations. Some researchers have suggested

that refuse is deficient in P (Pacey, 1989), but others have proposed that refuse contains sufficient P (Rees, 1980) (Rohrs et al., 1998). Barlaz, et al. (1989) observed phosphate depletion late in the decomposition process and recommended further research on a possible P limitation (Barlaz et al., 1990). Rhew and Barlaz (1995) reported dissolved phosphate concentrations of 0-5 mg P/L in leachate from MSW covered with soil, lime-stabilized sludge, or lime. These observations indicate that P decreases during refuse decomposition but it remains unclear whether it is limiting.

The second waste evaluated is a byproduct of the manufacture of corn-based polylactic acid. The manufacturer starts with a starch stream from a corn wet milling operation. After polymerization, a waste stream that contains lactic acid and glucose, henceforth referred to as burnt sugar (BS), requires disposal. It is a viscous mixture that represents a source of readily degradable organic carbon. It presented two challenges. First, its acidic pH is not compatible with methane production. Second, the readily degradable organic carbon will result in a rapid accumulation of short-chain carboxylic acids that would exert downward pressure on the pH.

The detergent wastes, one from fabric softener production and the second from detergent production, were acidic, suggesting that they would be problematic on the basis of pH alone. In addition, these wastes were expected to contain surfactants and possibly anti-microbial agents.

2 MATERIALS AND METHODS

2.1 Experimental Design

The overall objective of this research was to assess the effect of a number of non-hazardous industrial wastes on refuse decomposition. The three wastes evaluated, biosolids, BS and detergent wash water, are all candidates for disposal in landfills so an understanding of their potential impacts on refuse decomposition is of practical importance.

The effect of biosolids on refuse decomposition and dissolved P was evaluated in four sets of reactors including duplicate biosolids-only reactors (P1 to P2), refuse-only controls (P3 to P5), and reactors containing 10% and 20% biosolids on a wet weight basis (P6 to P8 and P9 to P11, respectively). These ratios are consistent with the ratio of biosolids to waste received at the landfill under study. Reactors were monitored for the presence of dissolved P (reactive, acid-hydrolyzable and total), concentrations of selected cations, and methane production.

While the biosolids were not expected to inhibit refuse decomposition, there was concern that the BS could inhibit decomposition based on its acidic pH and the potential for carboxylic acid production. A series of experiments were conducted to (1) determine the maximum amount of burnt sugar that could be added to decomposing refuse without reducing the pH on the basis of the acidic nature of the waste in the absence of biodegradation and (2) experiments to determine the maximum amount of BS that could be added to decomposing refuse without resulting in a pH decrease due to an inhibitory accumulation of carboxylic acids. For the first set of experiments, pH measurements were instantaneous, while in the second set of experiments, the leachate pH and methane production rates were measured over periods of weeks to identify an inhibitory BS addition.

Table 1 summarizes the reactors containing actively decomposing refuse that were operated to identify the maximum tolerable BS addition. BS was added as a solution to reactors BS3 and BS4 and as a layer in BS5 and BS6 to study BS dissolution and release to refuse.

Tests were terminated when methane production was permanently inhibited as a result of burnt sugar additions. In preliminary work, the BS was shown to dissolve when leachate was recirculated through a layer of the waste material.

Table 1: Description of burnt sugar reactors

Reactor	Description
BS1	Refuse control
BS2	Refuse control
BS3	Addition of a solution of BS dissolved in water to refuse
BS4	Addition of a solution of BS dissolved in water to refuse
BS5	Addition of a layer of BS over refuse
BS6	Addition of a layer of BS over refuse

The third waste requiring an assessment is actually two distinct wastes that are byproducts of fabric softener and detergent manufacturing, henceforth referred to as effluent softener and effluent soap, respectively. Initially, the compatibility of these wastes with anaerobic refuse decomposition was assessed using anaerobic toxicity assays (ATAs). The ATA is a batch test in which the ability of a methanogenic consortium to convert refuse to methane in the presence of another waste is assessed. Details have been described previously (Wang et al. 1994). A description of the contents of the serum bottles used in the ATA tests is presented in Table 2. The bottles were prepared with BMP medium, inoculum, DI water, ground refuse, and waste sample. An inoculum control and a refuse control were also prepared. Based on the ATA results, additional work was conducted in which detergent wastes were added to refuse decomposition reactors as for the BS. Reactors D1-D3 were operated as controls and reactors D4-D6 and D7-D9 received additions of effluent softener

and effluent soap, respectively. Steady initial methane production was an important consideration to assess the effect of waste addition, so each D reactor was filled with decomposing refuse mixed with shredded office paper. Tests were terminated when methane production was permanently inhibited as a result of waste additions.

Table 2: Contents of serum bottles designed to assess the methane potential and toxicity of fabric softener and detergent wastes.

	Medium (5X concentrate of BMP Medium) (mL)	Inoculum (mL)	H_2O (mL)	Ground Refuse (gm)	Liquid Sample (mL)
Inoculum Control	17	15	68	0	0
Refuse Control	17	15	68	0.5	0
1% dilution	17	15	67	0.5	1
10% dilution	17	15	58	0.5	10
30% dilution	17	15	38	0.5	30
50% dilution	17	15	18	0.5	50

2.2 Materials and Equipment

Refuse was incubated in 8-L polypropylene mason jars with a sealed screw cap (U.S. Plastics Corp., Lima, OH). Jars were modified for installation of the following: a leachate collection port, a water inlet, and a gas collection port. Each port accepted ¼" ID tubing. Gas was collected in foil-laminated tedlar gas bags fitted with a luer valve (Pollution Measurement Corp., Oak Park, IL). Leachate was collected in 2-L intravenous bags (Baxter Healthcare, Deerfield, IL). Assembled reactors were tested for leaks using a vacuum pump. A parts list for the reactors and a picture of an assembled reactor are presented in Table A-1 and Figure A-1, respectively.

Refuse collected in residential areas was obtained from the Holly Springs, NC transfer station and shredded with a slow-speed, high-torque shredder (Shredpax AZ-7H, Wood Dale, IL) so that most of the material was less than 2 cm by 5 cm. After shredding

twice, refuse was divided, mixed in totes, shoveled into 30-gallon trash bags, and transported to the laboratory. Refuse was stored at 4°C prior to use. Actively-decomposing refuse was obtained from a drum maintained in the laboratory. Biosolids from a secondary wastewater treatment plant process were aerobically digested with a solids retention time (SRT) of about 100 days and were then dewatered using a belt filter press. The SRT of the liquid train was about 50 days. Biosolids, BS, and the detergent wastes were obtained from Waste Management, Inc. All wastes were stored at 4°C prior to use.

2.3 Reactor Filling

For the biosolids research, two bags of refuse were selected randomly and mixed together to fill reactors P3-P11. Reactors P1 and P2 were filled with biosolids and about 4 L of deionized (DI) water to form a slurry. The average dry weight of biosolids in P1 and P2 was 245 g [standard deviation (sd) = 16.4]. For reactors P6 to P11, the appropriate amount of biosolids was mixed into refuse prior to filling each reactor. The reactors were filled in small compacted increments until a reactor was full. The average dry weight of refuse loaded into reactors P3 to P11 was 1840 g (sd=114). The average dry weight of biosolids in P6 to P8 and in P9 to P11 was 39 g (sd=0.9) and 84 g (sd=3.2), respectively.

For the burnt sugar research, each reactor was filled with 2 kg of wet refuse that was actively producing methane. The average dry weight of refuse loaded into the reactors was 822.5 g (sd = 3.2).

For the detergent research, each reactor was filled with 1.9 wet kg of actively decomposing refuse mixed with 0.6 dry kg shredded office paper. The shredded office paper was added to provide a substrate that would decompose at a steady rate (Eleazer et al., 1997).

The average total dry weight of the material loaded into the detergent reactors was 1390 g (sd=9.4).

As reactors were filled, composite samples were collected for moisture and solids analysis. After the reactors were filled, they were sealed and a gas bag was attached. Complete data on reactors and masses and moisture contents of fill material is presented in Table A-2.

2.4 Reactor Operation

Reactors were incubated under conditions designed to accelerate decomposition. This allowed rapid assessment of the effect of various treatments on decomposition. The incubation conditions included addition of deionized (DI) water to the refuse initially to ensure the generation of leachate for recirculation. DI water was added periodically to maintain about 500 mL leachate. Reactors were incubated at 35°C. Leachate from reactors P1-P11 and D1-D9 was neutralized with 5M NaOH to pH 8 and recirculated 4-5 times a week. Leachate samples were collected by inserting a syringe through a septum installed in the tubing. Leachate from BS1-BS6 was also recirculated 4-5 times a week but was not neutralized since determining the effect of BS on pH was of primary importance. Table 3 describes increasing BS solution additions that were made to reactors BS3 and BS4. Table 4 lists BS layer additions made to BS5 and BS6.

Table 3: Summary of burnt sugar solution additions to BS3 and BS4.

Spike	Day of Operation	Burnt sugar added (g/dry kg refuse)
1	10.9	3.3
2	14.7	7.9
3	21.8	12.9
4	27.8	17.5
5	33.8	21.3
6	42.7	24.5
7	48.6	35.0
8	54.8	42.0
9	60.9	47.5
10	67.9	87.4
11	76.8	131.2
12	87.9	196.7
13	112.7	295.1

Table 4: Summary of burnt sugar layer additions to BS5 and BS6.

Spike	Day of Operation	Burnt sugar added (g/dry kg refuse)
1	46.6	63.1
2	62.8	122.0
3	94.7	366.7

The total sodium concentration in the leachate from each biosolids reactor was calculated from the quantity of 5M NaOH added and the total volume of water. As this concentration approached 4000 mg/L, the reactors were neutralized with 5M KOH and the total K^+ concentration was then monitored. In the biosolids reactors, there was concern that the total concentrations of Na^+ and K^+ could be exhibiting toxicity. As the K^+ concentration approached 3100 mg/L, leachate was removed from the reactors and an equivalent quantity of DI water was added. Thus, over time, the leachate constituents were diluted. On day 112, methanogenic leachate was added to the reactors to promote the onset of methane production. A summary of leachate removal and DI water additions is presented in Table A-3 and the effect of dilution on various leachate concentrations is considered in the results.

2.5 Analytical Methods and Data Analysis

2.5.1 Methane Production

Gas volumes were measured in one of two ways dependent on the volume. For volumes below 5 to 10 L, gas bags were evacuated into an evacuated metal cylinder of known volume. The gas volume was calculated from the change in pressure in the cylinder. For larger volumes, gas was measured by water displacement. Gas bag contents were pumped into a calibrated plastic jug floating in pH 3 water (to prevent CO_2 dissolution). Gas concentrations were measured by gas chromatography (SRI Instruments, Torrance, CA). The injector and thermal conductivity detector temperatures were 100°C. The valve temperature was 90°C. Separation was obtained on a CTR 1 column (Alltech, Deerfield, IL) maintained at 75°C. The carrier gas was helium at 88 mL/min. 3 mL gas was injected into the 1 mL sample loop.

2.5.2 Leachate Composition

Leachate from the biosolids reactors was analyzed for dissolved reactive phosphorus (DRP), dissolved acid-hydrolyzable phosphorus (DHP), and dissolved total phosphorus (DTP). A flowchart of phosphorus fractions from Standard Methods is presented in Figure A-2. DRP (E in the figure) is comprised primarily of orthophosphate; DHP (F in the figure) is the amount of P remaining after DRP is subtracted from P determined via mild acid hydrolysis (DRHP; E+F in the figure); DTP (G in the figure) is composed of DRP, DHP, and organic phosphates. DRP has been recommended previously as a measure of the minimum bioavailable P (Reynolds and Davies, 2001).

Leachate was filtered and preserved under anaerobic conditions to prevent the oxidation of Fe(II) typically present in leachate to Fe(III) and the subsequent precipitation of Fe and sorption of PO_4 onto $Fe(OH)_3$ (Reynolds and Davies, 2001). Leachate samples were collected by syringe and injected into 10-mL uncoated Vacutainers (Becton-Dickinson, Franklin Lakes, NJ). Samples were filtered through 1.0 μm glass microfiber filters GF/B (Whatman Inc. USA) and 0.45 μm nylon syringe filters (Fisher Scientific, USA) in an anaerobic glove box with an N_2 (99%) and H_2 (1%) atmosphere (Coy Laboratory Products, Grass Lake, MI). After filtration, samples were stored at -20°C. In preliminary work presented in Table A-4, a significant difference in P and Fe was not found between samples treated aerobically and those treated anaerobically. DRP and DTP were measured by Hach methods 8048 and 8190, respectively. DHP was converted to PO_4 following Standard Method 4500-P B (APHA, 1998) and measured by Hach method 8048, where samples were acid hydrolyzed for 30 min in an autoclave and then neutralized. In preliminary work presented in Table A-5, all P analytical methods were verified by known additions of potassium phosphate, sodium pyrophosphate, and adenosine monophosphate to represent ortho-P, DHP, and organic P, respectively.

Samples for cation (Ca^{2+}, Fe^{2+}, Mg^{2+}, Al^{3+}, K^{+}, Na^{+}) analyses were collected and filtered anaerobically as for the P samples, acidified to pH <2, and stored at 4°C. Cations were analyzed by Inductively Coupled Plasma Emission Spectrophotometry (ICP). Samples for ammonia and chemical oxygen demand (COD) analyses were collected and filtered aerobically and were acidified to pH <2. The ammonia and COD samples were stored at 4 and -20°C, respectively. NH_4-N was analyzed by Standard Method 4500-NH3 H (APHA, 1992) using a QuickChem 8000 (Lachat Instruments, Loveland, CO). COD was measured

using a Hach kit (Hach Co., Loveland, CO) and a spectrophotometer set at wavelength 620 nm. Total organic carbon (TOC) concentrations were quantified by the non-purgeable organic carbon (NPOC) method using a Shimadzu Total Organic Carbon Analyzer (Model TOC-5000A).

For the BS research, volatile fatty acid (VFA) concentrations in leachate were measured. Acetic acid (ACS grade) was purchased from Sigma (USA), while propionic acid (99%) and n-butyric acid (99%), were purchased from Acros Organics (New Jersey, USA). All chemicals were used without further purification. Phosphoric acid (34% v/v) was prepared by diluting from 85% aqueous phosphoric acid solution (certified grade, Sigma). Stock standard solutions of VFAs were made by transferring 0.5 g of pure chemical to a 10 mL volumetric flask and filling it with HPLC grade methanol (Fisher Scientific) to volume. Stock solutions were stored at -20°C.

Leachate samples for VFA analysis were stored after collection at -20°C without any treatment. Before analysis, samples were thawed at room temperature and then homogenized with a Vortex mixer for 10-15 seconds. After 0.5 to 1 hr of settlement, the supernatant solution was filtered with 1.0 μm glass microfiber filters GF/B (Whatman Inc. USA) and 0.45μm nylon syringe filters (Fisher Scientific). Conditioned Dionex On-Guard H cartridges were used to clean up the filtrate. 2 mL of processed sample was then transferred to 10 ml vials with a screw magnet cap (Varian). 4 μL of 50g/L of 2-ethylbutyric acid was spiked into each vial as internal standard. 0.8 g NaCl and 0.2 ml of 30% (v/v) H_3PO_4 were added to each vial to increase the sorption of VFAs to SPME fiber.

Solid phase microextraction (SPME) was used to extract VFAs from leachate filtrate. Carbowax/divinylbenzene Stableflex fiber assemblies (70 μm, Supelco, PA,USA) were

utilized to adsorb and concentrate VFAs from leachate. Fiber-adsorbed VFAs were analyzed by a Varian CP3800 GC system with an automatic Varian Combi PAL injector. The detector was a Varian 2000 ion trap mass spectrometry. VFAs were separated using a DB-FFAP column (30m x 0.25mm x 0.85μm). During analysis, the agitator in the Combi PAL was maintained at 30°C. Before exposure to the SPME fiber, solutions were incubated to equilibrate for 10 min in the agitator. The clean fiber was exposed to the headspace above the leachate filtrate in the vials for 15 min at 30°C. After adsorption, the fiber was injected directly into the GC. The temperature of the injector was 220°C. The desorption time was 10 min. For the GC oven, the initial temperature of 50°C was held for 30 sec, increased to 100°C at a rate of 20°C/min, held at 100°C for 5 min, increased to 230°C at a rate of 8°C/min, and held at 230°C for 2 min. The carrier gas was He with a flowrate of 0.8 mL/min.

Electron ionization auto mode was used to collect the mass spectrum. Ions with an m/z ratio between 40 and 200 were trapped. The emission current was set at 10μA. The multiplier offset was 0 volts. Varian MS workstation software was used for data collection and handling. Prior to analysis, the mass spectrometry detector was autotuned. Qualitative identification of each VFA was based on the retention time and on mass spectrum match with standard solutions. Ion with m/z at 43 was used to quantify acetic acid and iso-butyric acid; m/z at 57, for propionic acid and iso-caproic acid; m/z at 60, for all other VFAs. The integrated abundance of the ions was used for quantitative analysis. Calibration curves with internal standard correction were used to calculate VFA concentrations.

In preliminary work, some samples were analyzed for VFA's using a similar procedure described in Appendix B.

2.5.3 Solids Composition

Dried samples were first ground in a Wiley mill to pass a 1 mm screen. Cellulose and hemicellulose were measured by acid hydrolysis of ground refuse samples followed by analysis of the hydrolyzed sugars by HPLC using a pulsed electrochemical detector (Petterson and Schwandt, 1991; Davis, 1998). Lignin was measured based on the loss on ignition at 550°C. Biochemical methane potential (BMP) assays were conducted as described previously (Wang et al. 1994). Composite samples of dried ground biosolids and refuse representing P reactor fill material were analyzed for total C, H, and N using a Perkin-Elmer 2400 CHN analyzer and for 20 other elements by ICP (University of Georgia Chemical Analysis Laboratory). BS was analyzed for carbohydrates by glycosyl composition analysis (University of Georgia Complex Carbohydrate Research Center) and for lactic acid using a Dionex ICS2500 with an AS11-HC column.

2.5.4 Data Analysis

All methane production data are reported as dry gas at STP. The ideal gas law was used to convert biogas volume collected in a gas bag to methane volume at STP:

$$PV = nRT$$

$$\frac{P_{STP}V_{STP}}{T_{STP}} = \frac{P_iV_i}{T_i}$$

$$V_{CH_4(STP)} = V_i\left(\frac{P_{SL} - VP}{760} * \frac{273.15}{T_i}\right) * \frac{\%CH_4}{100}$$

$$P_{SL} = P_A + 7.5$$

Where:

V_i = Measured biogas volume (L)
T_i = Measured temperature (°K)
P_i = Measured pressure (mm Hg)
P_A = Measured atmospheric pressure (mm Hg)
P_{SL} = Sea level pressure calculated by converting measured pressure by considering Raleigh, NC elevation and change in pressure with change in altitude (mm Hg)
VP = Calculated vapor pressure (mm Hg)
% CH_4 = Measured CH_4 composition by GC (% v/v)

Yields in reactors P6-P11 have been corrected for the methane potential of the biosolids. The following equation was used to correct yields:

$$\frac{mL\ CH_4}{dry\ g\ refuse} - \left(\frac{\frac{dry\ g\ biosolids}{reactor} * \frac{mL\ CH_4}{dry\ g\ biosolids}}{dry\ g\ refuse} \right) = \frac{corrected\ mL\ CH_4}{dry\ g\ refuse}$$

3 RESULTS AND DISCUSSION

An assessment of the influence of each waste on refuse decomposition is presented individually. The results for biosolids are presented first, followed by the results for the burnt sugar and detergent wastes.

3.1 Effect of Biosolids on Refuse Decomposition

The composition of the materials used in the biosolids reactors are summarized in the first part of this section, followed by data on methane production and leachate composition.

3.1.1 Materials Characterization

A characterization of the refuse and biosolids used in the P reactors is presented in Table 5. The cellulose, hemicellulose, and lignin content of refuse were similar to that reported previously for fresh refuse (Barlaz et al., 1990; Rhew and Barlaz, 1995; Price et al., 2003). The C:N:P ratio of the refuse was 100:1.8:0.6, which has less N and P than the optimal C:N:P ratio of 100:5:1 for anaerobic decomposition proposed by De Baere and Verstraete (1984) (Rohrs et al., 1998). Biosolids had about 8 times more N and P than refuse. The C:N:P ratios in P6 to P8 and P9 to P11, taken as a weighted average, were about 100:2.1:0.7 and 100:2.3:0.8, respectively. Complete results of the ICP-20 analysis are presented in Table A-6.

Table 5: P Reactor Fill Material Characterization

Parameter	Refuse used in P3-P11	Biosolids used in P1, P2, P6-P11
Moisture (wet weight basis)	29.0%	85.0%
Cellulose (dry mass)	46.3%	2.8%
Hemicellulose (dry mass)	10.1%	3.3%
Lignin (dry mass)	16.1%	21.7%
BMP (mL CH_4/dry g)	145.5	38.0
Volatile Solids	86.6%	66.0%
Total Carbon (dry mass)	43.7%	31.4%
Total Nitrogen (dry mass)	0.8%	4.5%
Total Phosphorus (dry mass)	0.3%	1.6%
Total Hydrogen (dry mass)	6.2%	4.7%
C:N:P Ratio	100:1.8:0.6	100:14.3:5.1

3.1.2 Methane Production

Gas production was monitored to evaluate the effect of biosolids addition on methane production rates and yields. The reactors exhibited the typical methane production rate curve described previously (Barlaz et al. 1990). After a lag phase, the methane production rate,

presented in Figure 1, increased sharply and then decreased asymptotically. Cumulative methane yields are presented in Table 6. Note that some corrected yields exceeded the refuse BMP. This suggests that the theoretical CH_4 potential of COD could be an inaccurate reflection of the true CH_4 potential; thus our analyses will be based on measured yields. P5, which produced no methane, was excluded from the analysis described below. No significant difference was found in the average maximum methane production rates among treatments. Although the average cumulative methane yield of the controls was greater than that of the 10% and 20% biosolids treatments, the difference was not significant.

As illustrated in Figure 1 and described in Table B-1, the reactors had lag times ranging from 67 days in P8 to 178 days in P6. P5 never produced significant methane. These lag times are in spite of efforts to neutralize the leachate described below. Biosolids did not have a significant impact on lag times. Potential explanations for the lag times will be discussed after the presentation of the leachate composition data. As the added biosolids were digested aerobically, they were not expected to have provided a seed of the anaerobic bacteria required for refuse methanogenesis.

Table 6: Cumulative methane yields in the biosolids reactors. Yields are as mL CH_4/dry g refuse at STP.

Reactor	Yield	Corrected Yield[a]
P3	141.3	187.5
P4	135.1	177.8
P6	144.6	182.6
P7	113.5	158.4
P8	126.2	140.7
P9	120.3	147.3
P10	120.0	154.5
P11	119.2	159.3

[a]The corrected yield includes the methane potential of leachate removed from each reactor. Yields were corrected assuming a conversion factor of 350 mL CH_4/g COD (Metcalf and Eddy, 1991).

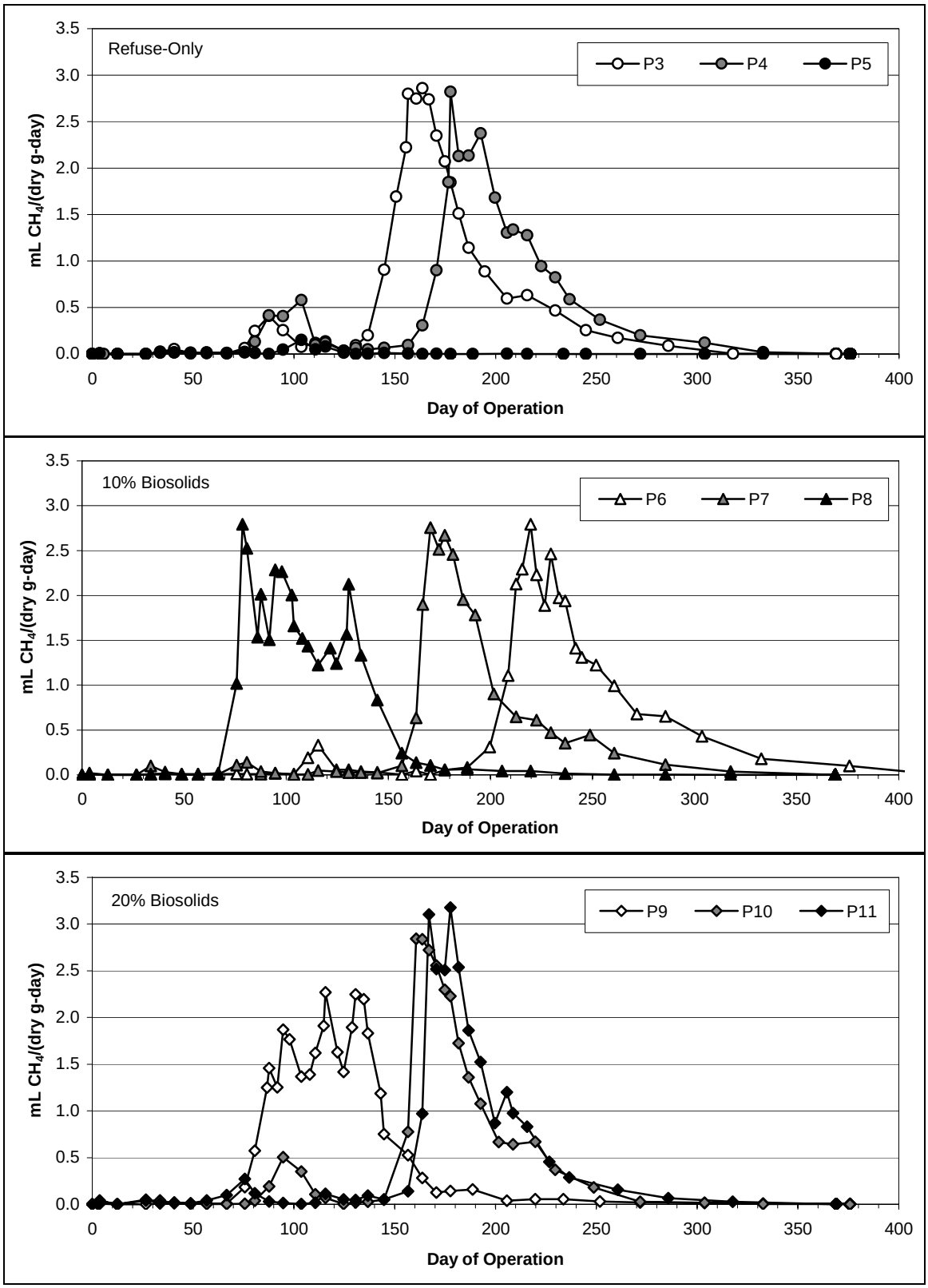

Figure 1: Methane production rates in the biosolids reactors, divided by treatment.

3.1.3 Leachate Composition

In the following sections, the behavior of leachate pH, phosphates, ammonia, salts, and selected cations over the different phases of refuse decomposition will be presented. The effect of biosolids on these parameters will be discussed. The effect of salt toxicity and leachate neutralization and recirculation strategies on lag times to the onset of methane production will also be examined. A final exercise is chemical equilibrium modeling of the reactors for comparison to measured parameters.

3.1.3.1 pH

pH is the most important parameter in refuse decomposition as methanogens are most efficient at a pH range of 6.8 to 7.4 and are inhibited at lower pHs. The leachate in each reactor was neutralized and recirculated daily in an effort to promote rapid onset of methanogenic conditions, but by day 40 the reactors had not yet neutralized and salts were approaching toxic levels from base additions. pH data for the biosolids reactors is presented in Figure 2, which also shows how the leachate neutralization and recycle (LN&R) strategy evolved over time. After day 40, the frequency of LN&R was reduced to weekly in an effort to decrease the impact of recirculating leachate. Leachate was also diluted several times between days 60 and 112 to decrease salt concentrations (dilution is discussed in more detail below).

pH and methane production rate (Figure 1) increased in reactors P3, P4, and P8 to P10, but not in P5 to P7 and P11 during the weekly LN&R period between days 40 and 90. Reactors P8 and P9 became neutral during this period. When daily LN&R was resumed

around day 90 to all reactors (for consistency) in an effort to increase constant acidic pH in reactors P5 to P7 and P11, the pH and methane production rate in reactors P3, P4, and P10, which had been increasing during weekly LN&R, decreased dramatically. The pH in reactors P5 and P6 also decreased. Daily LN&R was stopped as a result. Starting at day 110, the frequency of LN&R was decreased to weekly and was reduced further to once every 3 weeks at day 140. Between days 110 and 180, reactors P3, P4, P7, P10, and P11 neutralized. Reactor P6 neutralized several weeks later. Each reactor began consistent methane production once it became neutral. Reactor P5 never neutralized and never produced methane. The behavior of the reactors after the change in LN&R frequency from weekly to daily at day 90 gives strong evidence that LN&R was inhibitory to the developing methanogenic system in reactors P3, P4, and P10. This observation is discussed below.

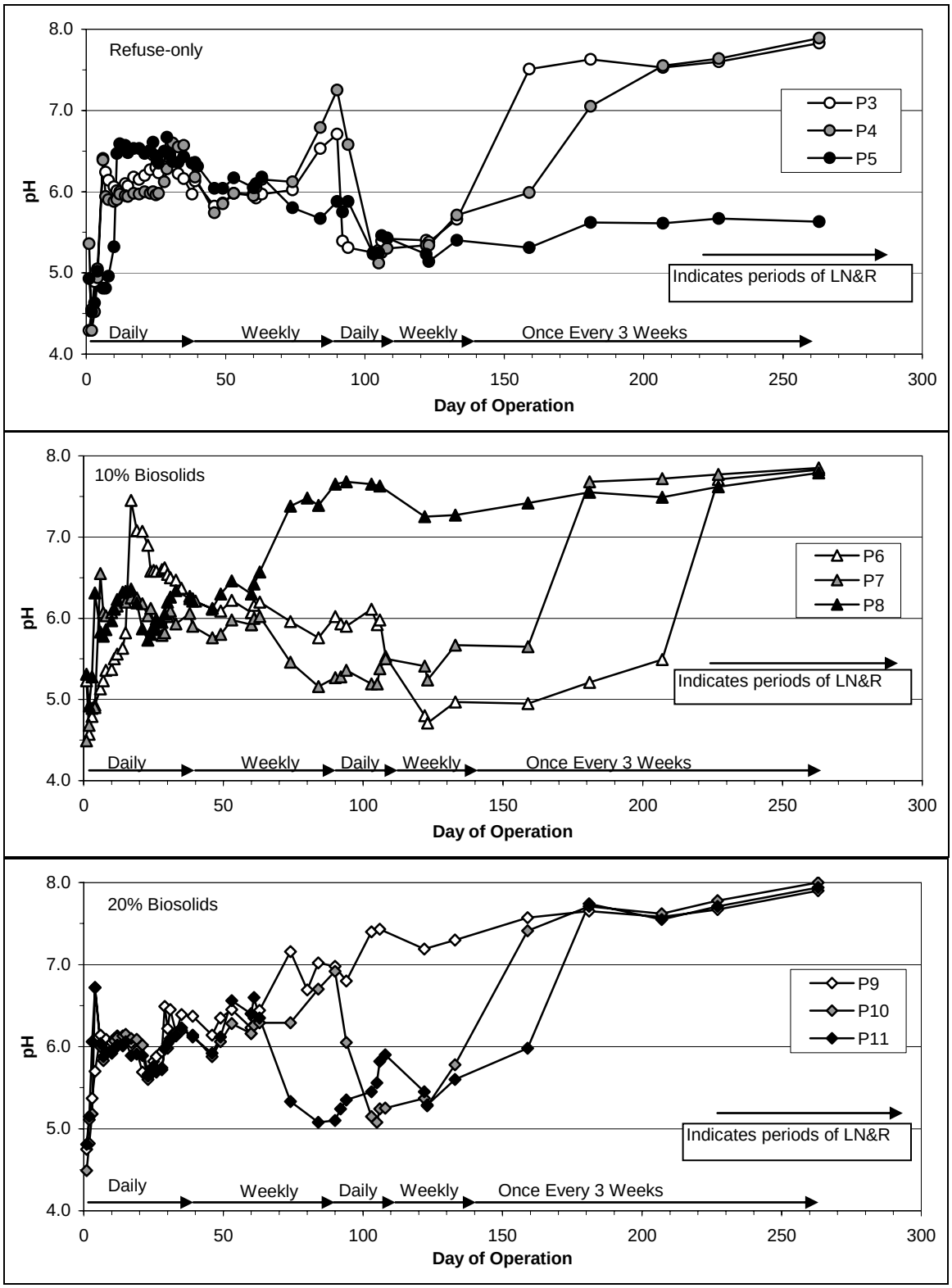

Figure 2: pH in the biosolids reactors, divided by treatment. The arrows indicate periods of leachate neutralization and recycle (LN&R) with frequency.

3.1.3.2 Phosphate Concentrations

Phosphate (reactive, acid-hydrolyzable and total) concentrations were monitored to evaluate the effect of biosolids addition on phosphate concentrations and to determine whether there were shifts in the form of phosphate during the refuse decomposition cycle. The DRP was generally greater than 10 mg PO_4/L in all reactors and decreased as methane production rates increased (Figure 3). All measurements are summarized in Table B-2 and representative data are presented in this section. DRP is plotted in Figure B-1 and Table B-3 presents a correlation matrix of DRP and the other measured leachate parameters. As illustrated for P8 and P9 in Figure 4, DRP and DTP concentrations tracked each other very closely. The similarity suggested that there would be very little DHP and this was evaluated in selected samples. DHP was calculated as the difference between DRHP and DRP. DHP was calculated for 12 samples and it averaged 9% of DTP (sd=24.8). The high variability in DHP results is likely because it was a small difference between two relatively large numbers. For example, in reactor P9 on day 39, DHRP was 104.1 mg PO_4/L and the DRP was 79.2 mg PO_4/L, which results in a DHP of 24.9 mg PO_4/L. In addition, there were some data where DHRP values were less than DRP or greater than DTP. Nonetheless, the close correspondence between the DTP and DRP indicate that DHP was not a significant component of the total P throughout the refuse decomposition cycle.

To evaluate whether the presence of biosolids increased the DRP concentration, DRP concentrations in each treatment were assessed using only those concentrations in which the leachate pH exceeded 7.3. The DRP data were segregated by pH because there was a negative correlation (r^2=0.35) between pH and DRP observed across all reactors (Figure 5).

This relationship is likely due to the effect of pH on the solubility of phosphate salts (e.g. hydroxyapatite). Working with the DRP concentrations in each reactor after its pH was greater than or equal to 7.3, the average DRP in the 20% biosolids treatment (avg=37.3, sd=18.6) was only greater than the control (avg=22.9, sd=14.5) and 10% treatments (avg=24.8, sd=12.7) at the 93% and 94% confidence levels, respectively. There was not a significant difference in DRP between the 10% and the control treatments. Below pH 7.3, a significant difference in DRP among the treatments was not observed. This is likely because pH was the dominant variable controlling the DRP concentrations and the effect of pH masked any effects attributable to biosolids.

The DRP was lowest in the reactors at the time of their maximum methane production rate (Figure 3 and Figure B-1). A comparison of the DRP at the time of the maximum methane production rate in each reactor showed that the average DRP in the controls (avg=1.9, sd=1.1) was significantly lower ($p<0.05$) than in the 10% biosolids (avg=11.8, sd=3.9) but not in the 20% biosolids (avg=13.6, sd=8.0). This does not indicate that P was limiting in the controls as the maximum methane production rate in all reactors were similar (Figure 1). DRP increased in all reactors after peak methane production. This increase is discussed below.

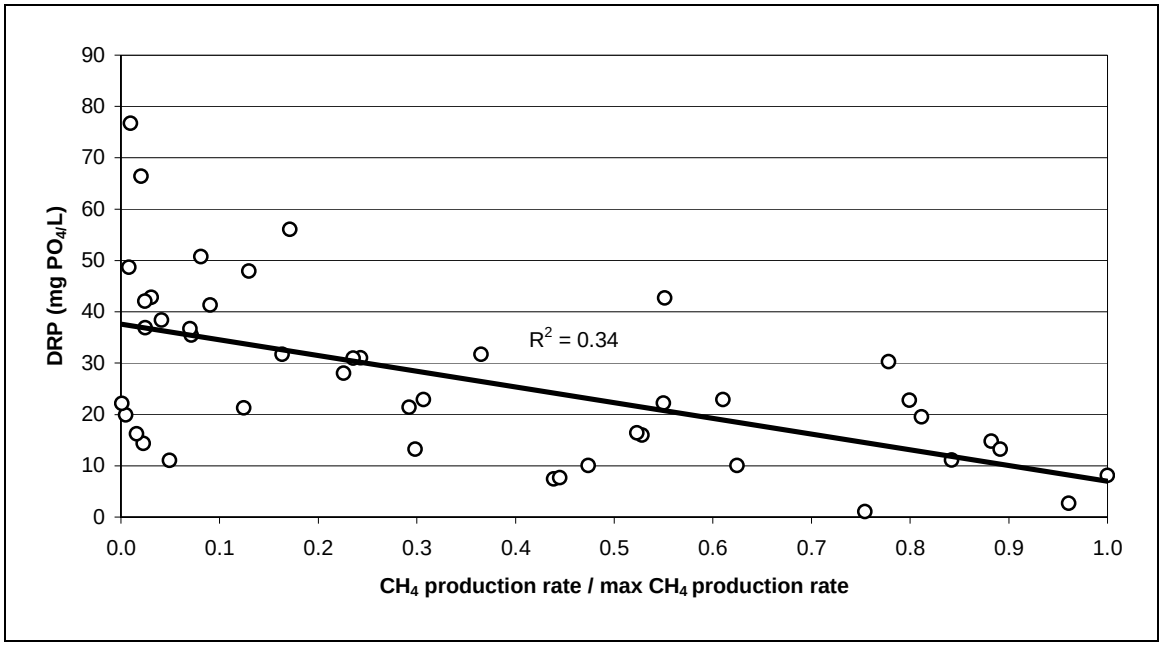

Figure 3: Correlation between DRP and CH_4 production rate in the biosolids reactors, excluding P5 as it never produced methane. Only data at pH≥7 is plotted to reduce the confounding effect of pH. The CH_4 production rate is normalized to the maximum CH_4 production rate. Correlations were $0.00 \leq r^2 \leq 0.97$ when reactors were considered individually (Figure B-2).

A

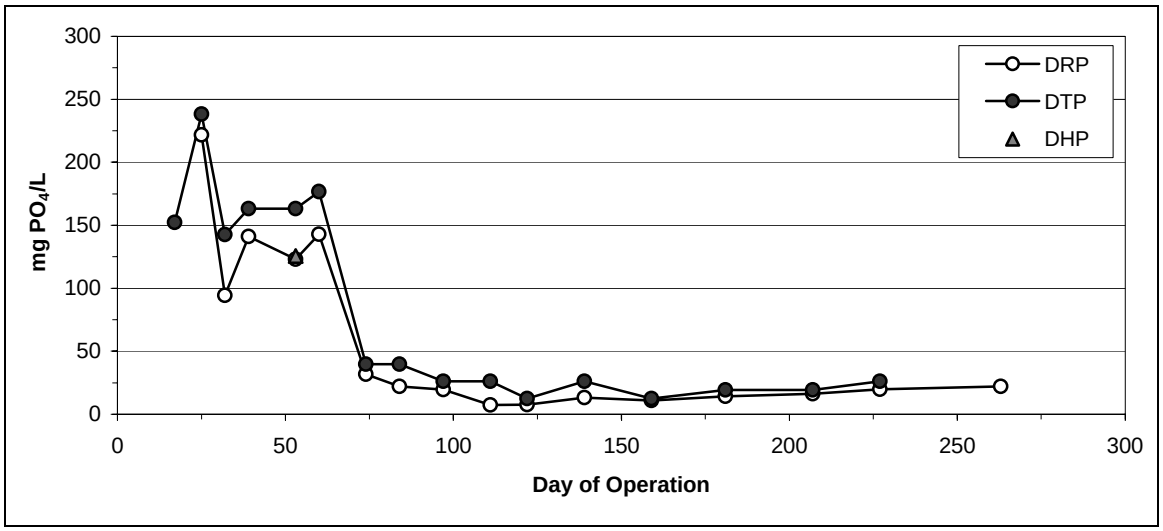

B

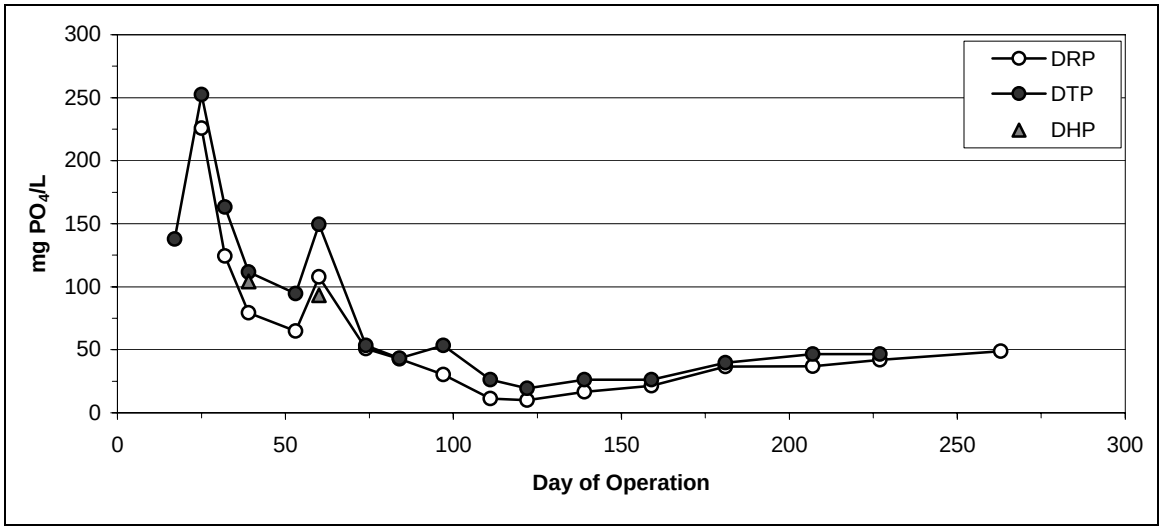

Figure 4: Dissolved reactive phosphorus (DRP), acid-hydrolyzable phosphorus (DHP), and total phosphorus (DTP) in reactors A) P8 and B) P9.

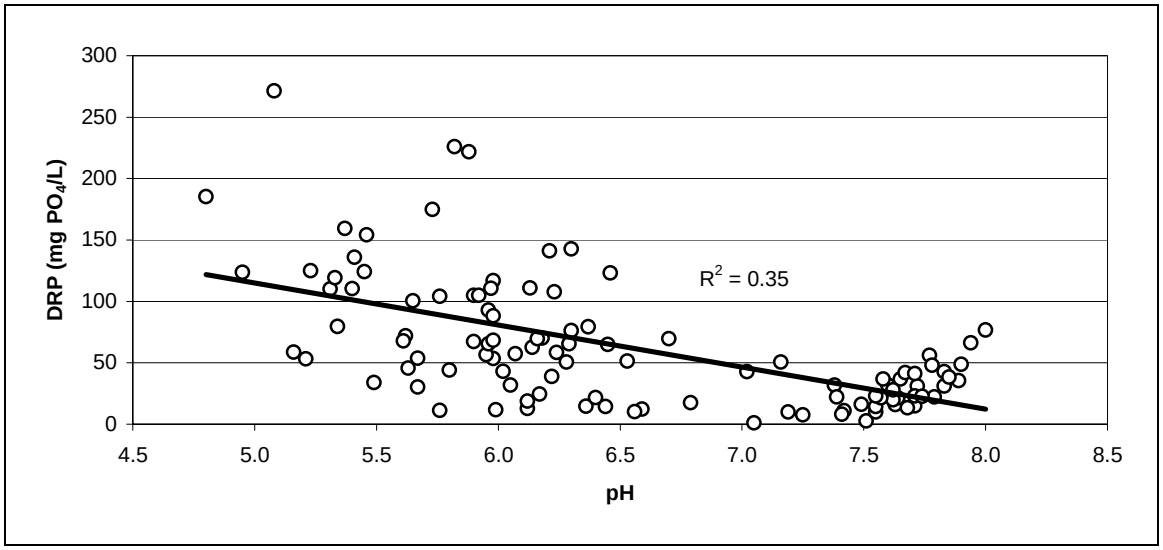

Figure 5: Correlation between pH and DRP in the biosolids reactors. When correlations are divided by reactors, then $0.33 \leq r^2 \leq 0.92$ (Figure B-3).

3.1.3.3 Ammonia Concentrations

Ammonia concentrations were measured to determine the effect of biosolids on ammonia. Plots of ammonia in the biosolids reactors are presented in Figure 6, which also includes plots considering dilution of the day 60 concentration only. Ammonia concentrations were primarily dependent upon dilution effects. Dilution decreased ammonia concentrations from 1800 to about 1000 mg N/L between days 60 and 74 and from 1000 to about 400 mg N/L between days 97 and 111. These levels are not considered to be inhibitory in anaerobic systems (Parkin and Owen, 1986). Also note the large ammonia increases (775 mg NH_4-N/L average) in reactors P8 and P9 after day 120. The cause for this increase is unknown, but it could be related to those reactors having neutralized first. Average ammonia concentrations of complete reactor runs were not found to be significantly different among treatments.

Concentrations were also analyzed after correction for dilution. In this case, the concentrations were increased to account for the added diluent, and these plots can be found in Figure B-4. When average corrected concentrations were compared among treatments, ammonia was found to be significantly greater ($p<0.05$) in the 20% biosolids reactors (avg=6599, sd=1596) than in the control (avg=5920, sd=1204) and 10% (avg=5852, sd=1167) treatments.

3.1.3.4 Phosphorus Increases after Peak Methane Production

Significant increases in DRP were observed in all reactors following peak methane production (Figure 3 and Figure B-1). In reactors P3 to P11, excluding P5, DRP increased from the lowest measured concentration by an average of 37 mg PO_4/L (sd=17). One possible explanation for these increases is that P was released back into solution as microbial populations lysed due to decreasing substrate.

To evaluate cell lysis as an explanation for the observed increases in PO_4, potential release of PO_4 back into the leachate was estimated. A population of 10^9 total fermenters/dry g refuse at the time of maximum methane production was assumed (Barlaz et al., 1989) and it was further assumed that this population subsequently experienced an order of magnitude population decrease. A typical 1 μm cell weighs about 2.8×10^{-13} dry g (Madigan et al., 2002) and the P content is 1 to 3% (Jjemba, 2004). The lysis of 90% of the total fermenter population would result in an increase of 4 to 11 mg PO_4/L. The DRP concentration at the time of maximum methane production was 1 to 13 mg PO_4/L so an increase of 4 to 11 mg/L could partially explain the 37 mg/L DRP concentration increase.

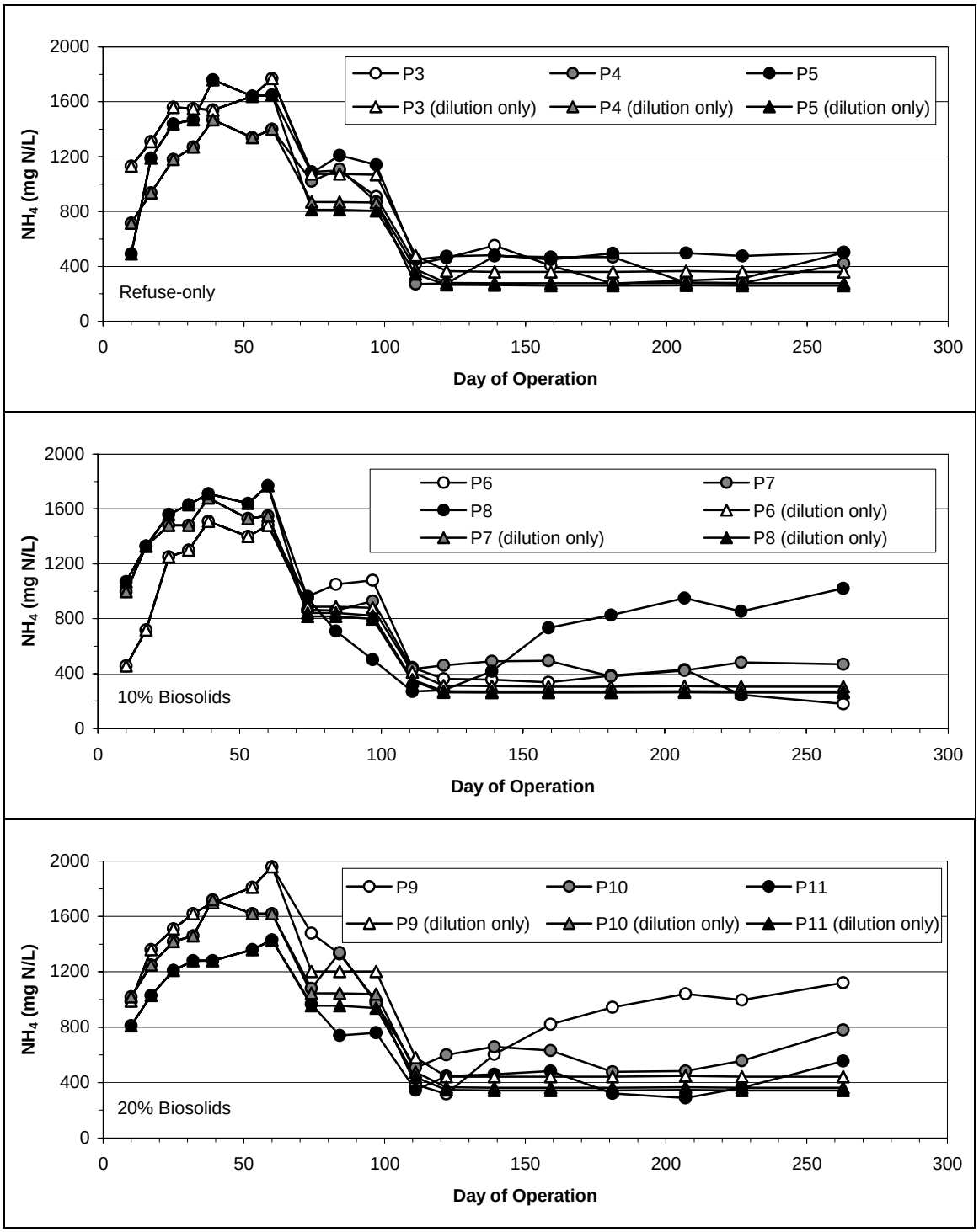

Figure 6: Ammonia concentrations in the biosolids reactors, divided by treatment. The plots labeled dilution-only only consider dilution of the measured concentration at day 60 based on known leachate removals and DI water additions. A schedule of the dilutions is presented in Table A-3. Plots corrected for dilution are presented in Figure B-4.

3.1.3.5 COD

Trends in the dissolved COD concentrations in reactor leachate were typical of what has been reported in previous studies (Rhew and Barlaz, 1995). The COD increased to around 55000 mg/L prior to the onset of methane production and exhibited a steep decrease thereafter. After the reactors neutralized, the COD decreased to less than 5000 mg/L. COD plots are presented in Figure B-5.

3.1.3.6 Sodium and Potassium Concentrations

To evaluate Na and K concentrations that were tolerated, the Na and K concentrations at the time of the maximum methane production rate in each reactor were compared (Figure 7). Reactors P4, P7, P10, and P11 had similar salt concentrations during active methane production and the maximum concentrations were 4100 mg Na/L and 800 mg K/L in P4. The maximum methane production rate in these reactors were comparable to those in P8 and P9, which had considerably lower maximum salt concentrations; 2900 mg Na/L and 1400 mg K/L during active methane production. The maximum methane production rates measured here are comparable to those reported in previous studies (Rhew and Barlaz, 1995; Eleazer et al., 1997) although salt concentrations in the previous studies were likely lower. While there are not sufficient data to identify the concentration of Na and K at which inhibition may have occurred, the data do serve to identify salt concentrations at which methane production rates were comparable to literature values. For reference, McCarty (1964) reported that Na and K concentrations of 3500 to 5500 and 2500 to 4500 mg/L, respectively, were moderately inhibitory in anaerobic systems (Parkin and Owen, 1986). McCarty (1961) also showed that acclimation was possible and that the addition of antagonistic cations can reduce, and even

eliminate, the toxicity caused by the light metal cations (Parkin and Owen, 1986). K is an antagonistic cation to Na (Parkin and Owen, 1986).

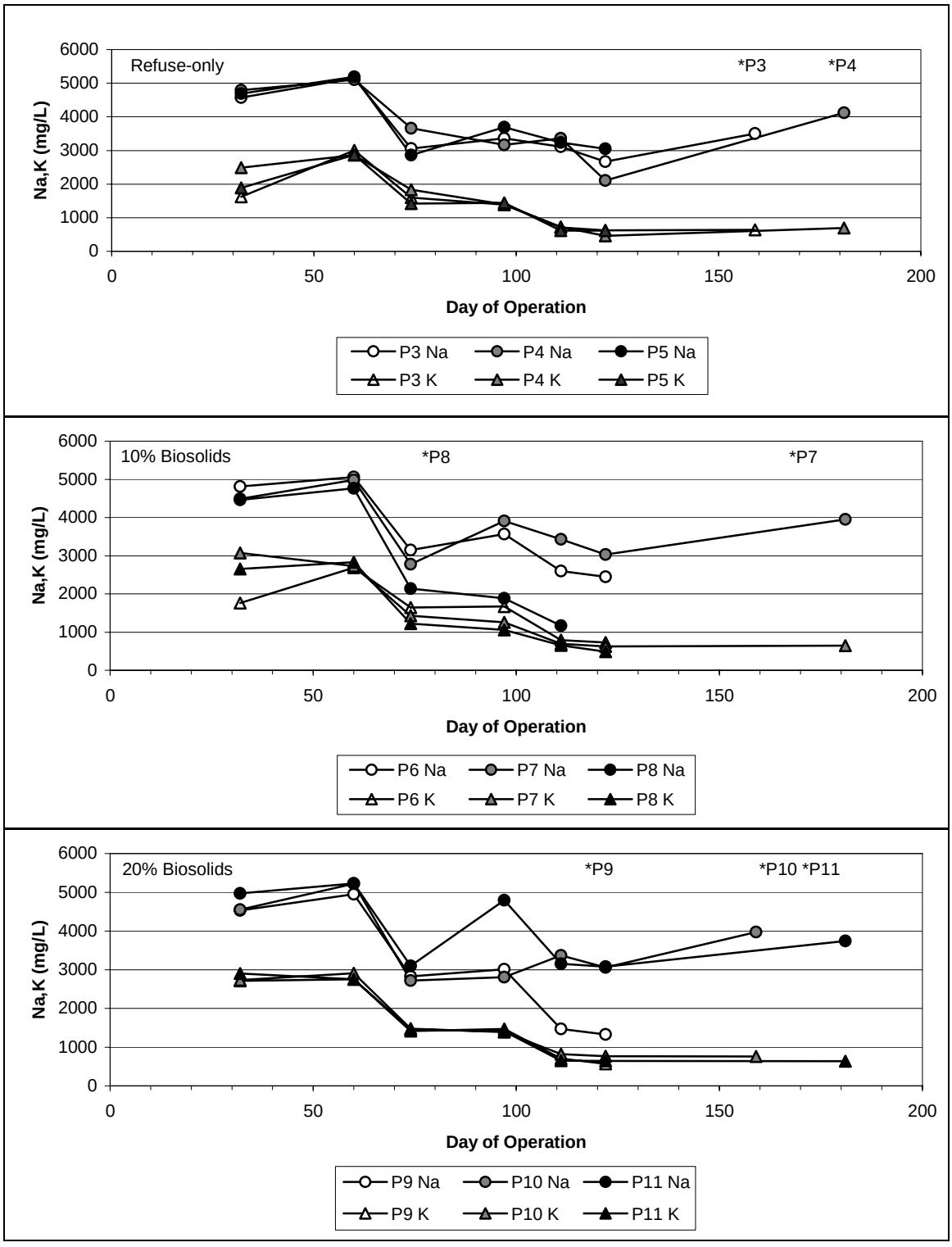

Figure 7: Salt (Na, K) concentrations in the P reactors, divided by treatment. The * followed by the reactor name denotes the day when the maximum methane production rate was measured in that reactor. A schedule of leachate dilutions is given in Table A-3.

3.1.3.7 Concentrations of Calcium, Iron, Magnesium, and Aluminum

Cations were measured to determine their relationship to pH, DRP, and to each other. Plots of Ca^{2+}, Fe^{2+}, Mg^{2+}, and Al^{3+} are presented in Figures B-6, B-7, B-8, and B-9, respectively. Cations were selected based on their known presence in landfill leachate and by their involvement in important solubility reactions. Negative correlations between pH and Ca^{2+} (r^2=0.47), Fe^{2+} (r^2=0.31), and Mg^{2+} (r^2=0.30) were observed as would be expected on the basis of solubility. There was not enough pH variation in the available Al^{3+} data to perform a linear regression. Linear regressions are presented in Figure B-10. Cation concentrations were largely dependent upon pH and dilution effects, and were not significantly impacted by the presence of biosolids. No relationship was observed between DRP and Ca^{2+}, Fe^{2+}, Mg^{2+}, or Al^{3+}. A correlation ($0.66 \leq r^2 \leq 0.94$) between Mg^{2+} and NH_4^+ was observed (Table B-3), but this is likely attributable to their similar response to dilution (compare Figure B-8 to Figure 6).

Soluble Ca^{2+}, Fe^{2+}, and Mg^{2+} concentrations decreased with increasing pH and with leachate dilutions to about 100, 10, and 20 mg/L, respectively, after reactors neutralized. Ca^{2+} concentrations began above 1000 mg/L in most cases, decreased to at most 50% of the initial concentration by day 40, decreased slightly again due to dilution (except P11, which increased dramatically from 902 to 1760 mg/L between days 60 and 97), and decreased to about 100 mg/L after leachate neutralized. The initial high Ca^{2+} concentrations and subsequent rapid decrease could indicate that the initial DI water addition leached calcium from the solid refuse into solution, followed by calcium precipitation. Fe^{2+} showed a trend where concentrations began low (<100 mg/L in most reactors before day 50), increased significantly in the acid phase in reactors (except P8 and P9) even during leachate dilution

(P4 and P6 reached maximums of 330 and 480 mg Fe/L, respectively), and decreased to about 10 mg Fe/L after neutralization. Reactors P4 and P6, which remained acidic for long periods of time, showed accumulations of Fe^{2+} until they neutralized, while P8 and P9, which neutralized first, did not show Fe^{2+} accumulation. Fe^{2+} accumulation in P4 and P6 could be due to slow release of Fe^{2+} at low pH into the system from iron-containing solids. The concentration profiles of Mg^{2+} were largely dependent on dilution and were very similar among all reactors. Mg^{2+} was not observed above 160 mg/L. Dissolved Al^{3+} was measured starting on day 139, and concentrations remained below 10 mg/L with no observed differences among treatments or variations over time.

3.1.3.8 Analysis of Lag Times

The objective of this section is to analyze the measured lag times in the reactors. As described above, the reactors had lag times ranging from 67 days in P8 to 178 days in P6. Two potential explanations for the lag times are inhibitory salt concentrations (Na, K) and disturbance of developing methanogenic zones due to leachate recirculation. As described in the previous section, the methane production rates measured in this study were comparable to previous reports and the behavior of the methane production rates at the highest calculated salt concentrations does not support significant salt inhibition. However, the pH and methane production data do support the idea that the development of methanogenic zones may have been inhibited.

By day 60, the pH in P3 to P11 was still acidic (Figure 2) and salt concentrations had increased to potentially inhibitory levels (5000 mg/L Na, 3000 mg/L K) from the daily additions of 5M NaOH and KOH for leachate neutralization (Figure 7). To alleviate

potential salt inhibition, reactor leachate was removed and diluted several times to decrease salt levels. A schedule of leachate dilution is given in Table A-3. P8 and P9 subsequently neutralized and began producing methane, but the other reactors remained acidic.

It was then hypothesized that leachate recirculation may have been inhibiting the development of a healthy methanogenic ecosystem by disturbing colony development. This is based on studies by Stroot et al. (2001) and McMahon et al. (2001), who concluded that a reduction in mixing improved anaerobic digester performance and that "mixing appears to inhibit the syntrophic oxidation of volatile fatty acids, possibly by disrupting the spatial juxtaposition of syntrophic bacteria and their methanogenic partners" (McMahon et al., 2001). The methane production rates and leachate pH data (Figures 1 and 2, respectively) suggest that leachate recirculation induced mixing which was detrimental to the developing methanogenic system. These observations also support the reaction front hypothesis of methanogenic zones that develop in anaerobic environments and expand as acids are consumed (Martin et al. 2003). Recirculation of leachate could have disturbed those developing zones, especially since fresh refuse, which would contain few microorganism seed bodies, was used.

3.1.4 Equilibrium Modeling with MINTEQ

A geochemical equilibrium model, Visual MINTEQA2 (version 4), was used to model several of the biosolids reactors to compare measured DRP to equilibrium phosphate concentrations estimated by MINTEQ. Measured cation (Al^{3+}, Ca^{2+}, Fe^{2+}, K^{+1}, Mg^{2+}, Na^{+1}, and NH_4^{+1}), anion ($PO4^{3-}$), and pH data were input to the model. An atmosphere of 0.5 atm CO_2 was assumed, from which carbonate concentrations could be calculated. The model was

used without consideration of sorption or humic matter. Minerals determined by initial runs of the model to be oversaturated were added as infinite solid phase inputs and the model was rerun. The model consistently determined that the minerals hercynite [$FeAl_2O_4$], hydroxyapatite [$Ca_{10}(PO_4)_6(OH)_2$], ordered dolomite [$CaMg(CO_3)_2$], siderite [$FeCO_3$], and calcite [$CaCO_3$] were important at neutral pH.

Table 7 presents the inputs and outputs of a typical model run which represents reactor P3 on day 159. In this case, MINTEQ suggested that the system was oversaturated in Al^{3+}, Ca^{2+}, Fe^{2+}, and Mg^{2+}, but not in PO_4^{3-}. One potential explanation for the supersaturation is that humic matter increased cation concentrations by complexation. Results from additional model runs are presented in Table B-5. The model proved to be a fair predictor of phosphates in the refuse system and the model results support the high measured P concentrations. At neutral pH, the model often determined the system to be supersaturated in Ca^{2+}, Fe^{2+}, and Mg^{2+}. This exercise demonstrates the usefulness of MINTEQ as an assessment tool for modeling chemical behavior in MSW leachate.

Table 7: Equilibrium modeling in MINTEQ of P3 on day 159. The input pH was 7.51 and the model-calculated charge difference was 21.5%. Outputs from the model used to calculate equilibrium concentrations are presented in Tables B-6 and B-7.

Component	Inputs (mg/L)	Outputs (mg/L)[a]	Free Form (mg/L)
Al^{3+}	3.2	0.0	
Ca^{2+}	137	2.5	1.0 (Ca^{2+})
CO_3^{2-}	(0.5 atm CO_2)	18519.6	
Fe^{2+}	19	0.0	
K^+	636	636.0	
Mg^{2+}	21	0.8	
Na^+	3500	3501.5	
NH_4^+	520.7	519.6	
PO_4^{3-}	2.66	67.2	41.9[b] (H_3PO_4, $H_2PO_4^-$, HPO_4^{2-}, PO_4^{3-})[b]

[a]Total equilibrated mass distribution as mg/L component
[b]Free forms of phosphate comprised about 62% of the total dissolved equilibrated mass of phosphorus

3.1.5 Conclusions

Overall conclusions of the biosolids research are presented below:

- Aerobically-digested biosolids were compatible with refuse decomposition but the biosolids did not increase maximum methane production rates and yields or reduce lag times to the onset of methane production. There is some evidence that biosolids increased DRP and NH_4, but this had no observed effect on maximum methane production rates.
- DRP and DTP profiles are similar during refuse decomposition, indicating that DHP is not a significant form of phosphate.
- DRP was lowest (1 to 13 mg PO_4/L) during maximum methane production, but this did not indicate that the system was phosphorus-limited as the maximum methane production rates in all reactors were similar to each other and to previous studies.
- DRP increased from its concentration at the time of maximum methane production by an average of 37 mg PO_4/L (sd=17). One possible explanation for this increase is that P was released back into solution as microbial populations lysed due to decreasing substrate.
- The maximum tolerated Na and K concentrations during active methane production were at least 4100 mg Na/L and 800 mg K/L, respectively. These levels were not considered inhibitory as other reactors in the study with lower Na and K levels exhibited similar maximum methane production rates and these rates were comparable to those reported in previous studies.

- A shift in LN&R frequency from weekly to daily appeared to decrease the pH in reactors P3, P4, and P10. LN&R may have inhibited the development of a healthy methanogenic ecosystem by disturbing developing zones.

3.2 Effect of Burnt Sugar on Refuse Decomposition

The composition of the BS is summarized in the first part of this section, followed by data on the dissolution, pH buffering, and refuse decomposition experiments.

3.2.1 Materials Characterization

The primary constituents of the BS were 0.73 g lactic acid/dry g and 0.12 g glucose/dry g. It also contained small amounts of other sugars. Complete results of the sugar and lactic acid analyses are presented in Table A-7 and A-8. The COD of the BS was 1.23 g COD/dry g and it had a pH of 3-4 when 10 g/L was dissolved in water.

3.2.2 Abiotic Dissolution and pH Buffering

Prior to an assessment of the biodegradation characteristics of BS, experiments were conducted to confirm that the material would dissolve into leachate and to determine the amount of BS that could be added to well-decomposed refuse without decreasing the pH below about 6.5. To assess dissolution, 150 g of BS was poured over sand in an 8-L jar to form a layer. Sterilized leachate, in which 65 g/L sodium azide was dissolved to prevent microbial regrowth, was recirculated over the layer daily. At 35°C, about 75% of the BS dissolved into the leachate within 4 days based on COD recovery while at 22°C, 65% of the

BS dissolved in 43 days (Figure B-11). The percent dissolution was calculated from the COD of the mass of BS added and the COD recovered in leachate.

The pH of well-decomposed refuse immediately after sugar addition was 7.13 to 6.41 at BS additions of 11 and 21.9 g/dry kg refuse, respectively (Table B-8). Thus, on the basis of the buffer capacity alone, with no consideration for the refuse microbial community to consume acidic substrate, a BS addition above perhaps 1.5% by weight may result in an inhibitory pH. In subsequent experiments presented next, where BS was added to actively decomposing refuse, the pH was monitored in consideration of microbial substrate consumption.

3.2.3 Refuse Decomposition Experiments

The refuse decomposition experiments were monitored to determine the behavior of actively decomposing refuse after BS additions of increasing concentration. Methane production rates for the control reactors and the reactors receiving additions of dissolved BS are presented in Figure 8. The corresponding pH data are presented in Figure 9. The pH of the leachate in the reactors that received BS remained neutral through spike 10 (87.4 g BS/dry kg refuse) which is considerably higher than the 21.9 g BS/dry kg addition that was shown to decrease the pH to 6.41 in the absence of biodegradation (Table B-8). Thus, the decomposing refuse was able to accommodate more BS than determined based on the results of the pH experiment. This suggests that the buffer capacity of the refuse was able to maintain the pH at a level from which the microbial community could recover rapidly from the shock of the BS addition. This view is supported by the methane production data and the volatile fatty acid (VFA) data (Figure 10). After a BS addition, the methane production rate

increased consistently for 2 to 3 days relative to the controls. VFAs increased after BS additions and decreased thereafter as BS was converted to CO_2 and CH_4.

With subsequent BS additions a more pronounced drop in pH was observed. For example, after spike 11 (see Table 3 for spike amounts) the pH decreased to 6.6 and then recovered 6 days after the spike. A lag to maximum methane production was also observed. The lag time increased with spike 12 when the pH decreased to 5.8 and did not become neutral for 19 days. After spike 13, the pH decreased to 4 and never recovered. Methane production also dropped to negligible levels, indicating inhibition of methanogens. pH and methane production were monitored for about 55 more days with no changes, and the experiment was terminated. Thus, spike 12 defined the maximum amount of BS that could be attenuated in this system.

An accumulation of COD was also observed as the BS additions increased (Figure 11). The day 117 COD reflects the addition of spike 13 that was not degraded. The amount of COD that was added in spike 13 corresponds to a leachate COD of 116000 mg/L which is comparable to the leachate COD of about 100000 mg/L that was measured. Operating concurrently, the COD in the control reactors decreased from 5000 to 3000 mg/L while the COD in reactor BS4 was about 22000 mg/L even when it was degrading the added BS. Converting acetic, propionic, and butyric acid concentrations to COD at days 110 and 113 (before spike 13) accounts for less than 5% of the measured COD in BS4. The measured sugar and lactic acid concentrations (Table A-9) could account for 79% of the BS COD. Assuming that the remaining 21% of the BS COD was recalcitrant, this would explain an accumulation of 52000 mg/L of COD in the leachate after spike 12.

VFA spikes also intensified with increasing BS additions. After spike 13, VFAs increased and remained relatively constant until the reactors were terminated, indicating that there was some fermentative activity initially, but that fermentation became inhibited after day 117. The VFA levels after day 117 only account for about 10% of the COD added to the system with spike 13, indicating that a large amount of unmetabolized burnt sugar remained. High levels of propionic acid were observed immediately after BS additions (Figure 10). One explanation for this is that the lactic acid in the BS was being converted to propionic acid. Zellner et. al (1994) reported conversion of lactate to propionate by an anaerobic mixed culture in a fluidized bed reactor. The researchers found that an initial lactate concentration of 3600 mg/L favored the growth of propionate-forming *Clostridium* sp. Zellner at al. (1994) also reported that *Clostridium propionicum* ferments lactate through the following reaction:

$$3 \text{ lactate} \rightarrow 2 \text{ propionate} + \text{acetate} + CO_2 + H_2O$$

Samples have been collected for DNA fingerprinting and more information will be available on the presence of propionate-forming species in the future.

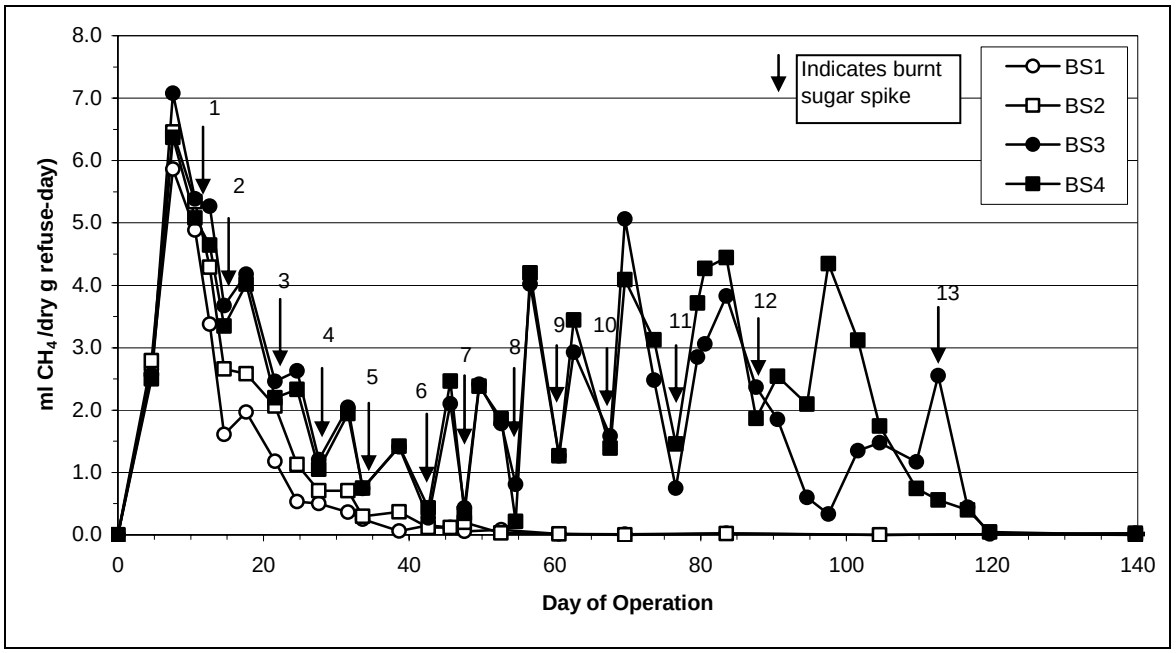

Figure 8: Methane production rates in control reactors and reactors that received BS solution additions. The numbers above the arrows refer to spike additions described in Table 3.

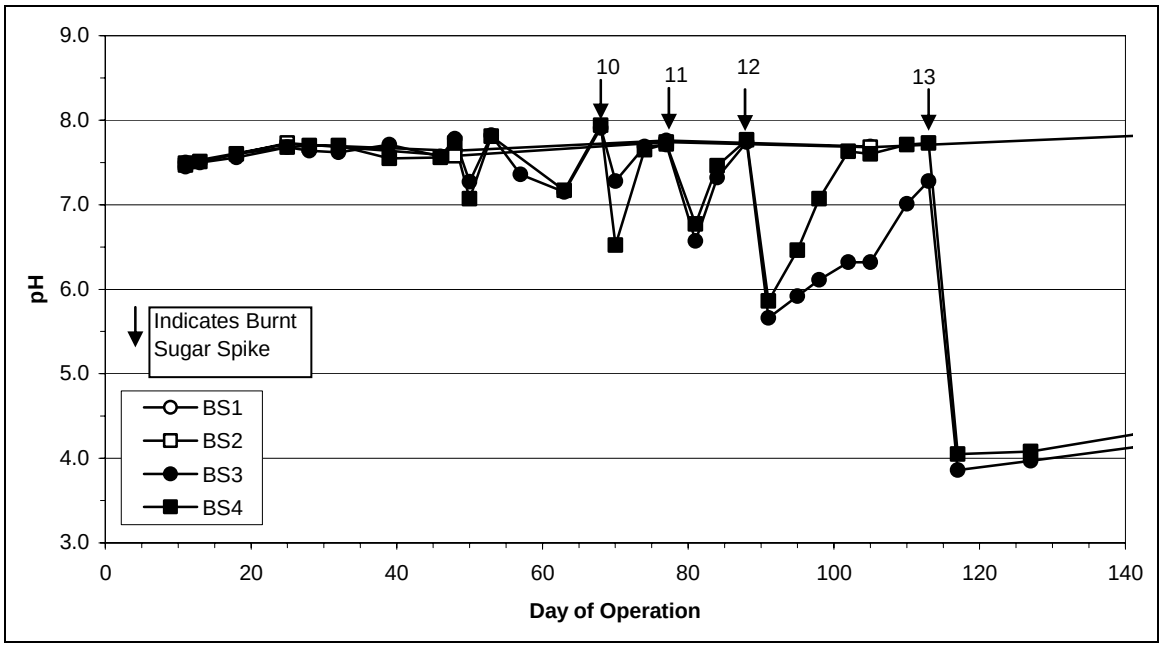

Figure 9: pH of control reactors and reactors receiving BS solution.

A

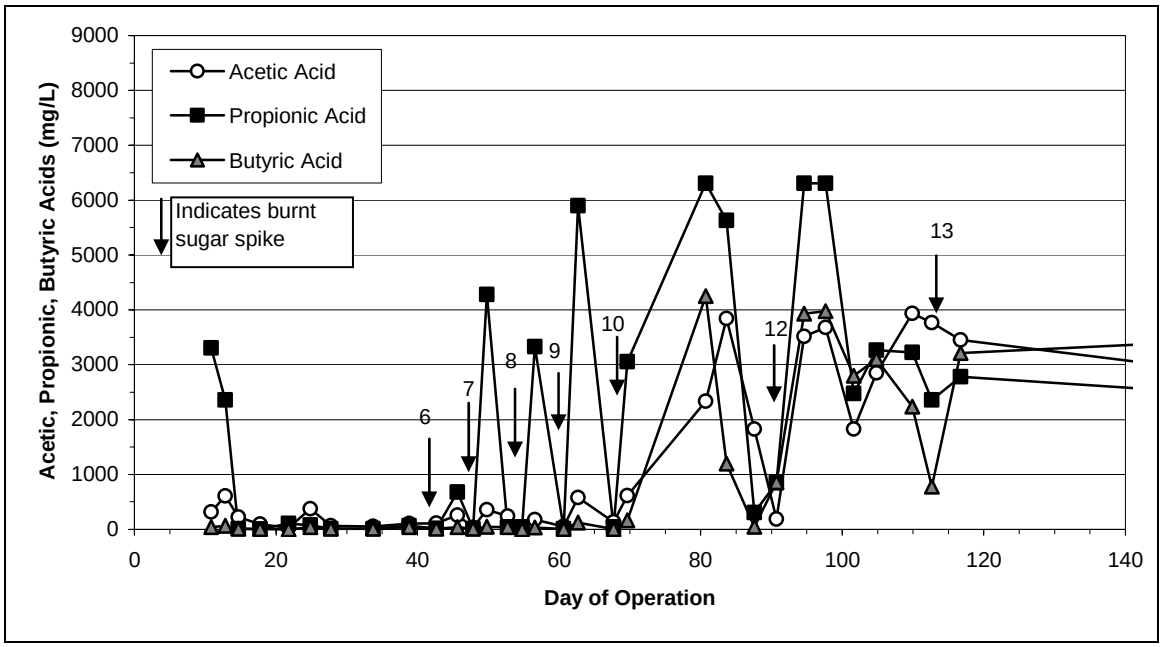

B

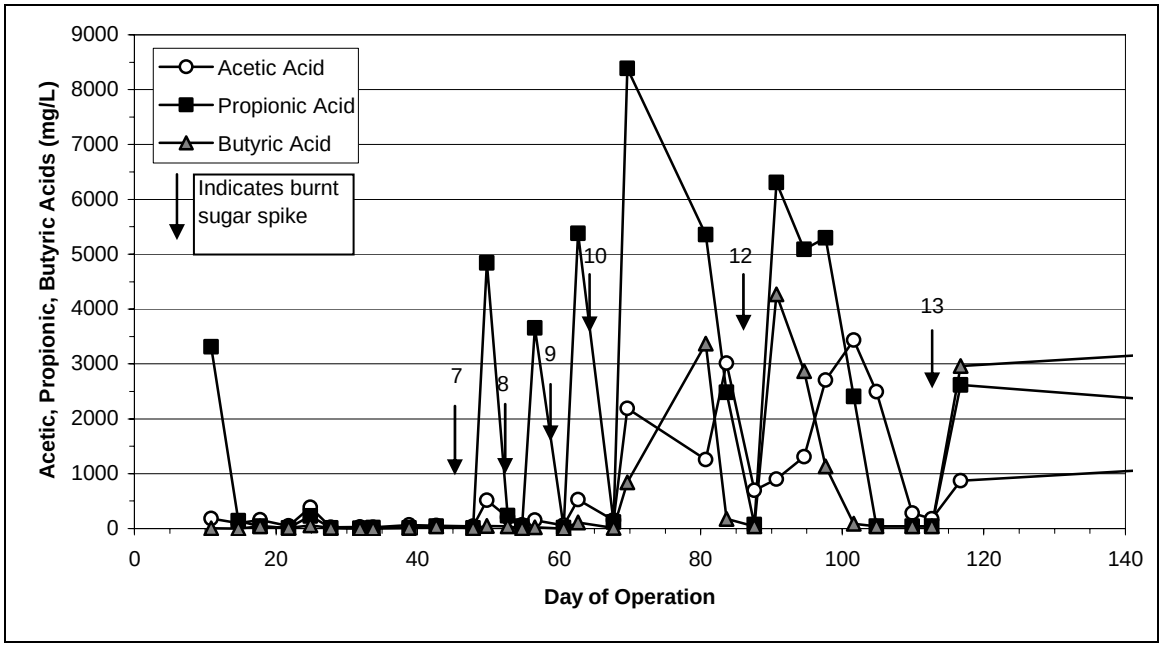

Figure 10: VFA's (acetic, propionic, and butyric acids) in reactors A) BS3 and B) BS4. These plots incorporate data from two VFA analysis methods. Tables presenting data used to plot these graphs are presented in Tables B-11 and B-12.

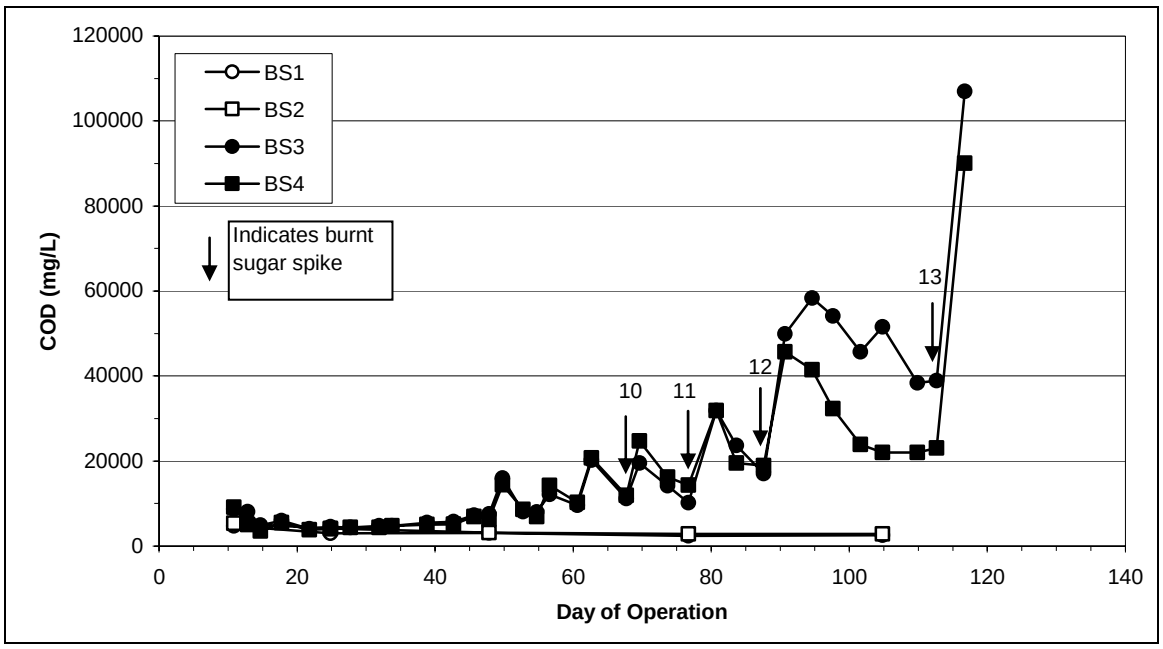

Figure 11: COD concentrations in controls and reactors receiving BS solution.

A mass balance on methane potential was performed on BS3 and BS4 to assess the amount of the added BS that could be accounted for. The measured CH_4 attributable to the BS addition was the difference between the measured CH_4 in the BS and control reactors. This value was added to the CH_4 potential of the accumulated COD in the leachate plus the COD of the leachate removed during sampling, using a conversion factor of 350 mL CH_4/g COD (Metcalf and Eddy, 1991). The sum of these values was compared to the CH_4 potential of added BS which was calculated from its COD (1.23 mg COD/gm BS). The result was that 74.5% and 73.9% of the CH_4 potential added as BS was recovered in BS3 and BS4, respectively. Detailed calculations are presented in Table B-13.

One final experiment was conducted in which layers of solid BS were added to the top of reactors filled with decomposing refuse. For the first and second additions, the pH remained neutral, and the methane production rate increased (Figure 12). After the third

addition, the reactors failed. (Masses of layer additions are presented in Table 4). Methane production dropped to zero and the pH dropped to 4. The reactors remained in this condition for 70 days, after which the experiment was terminated.

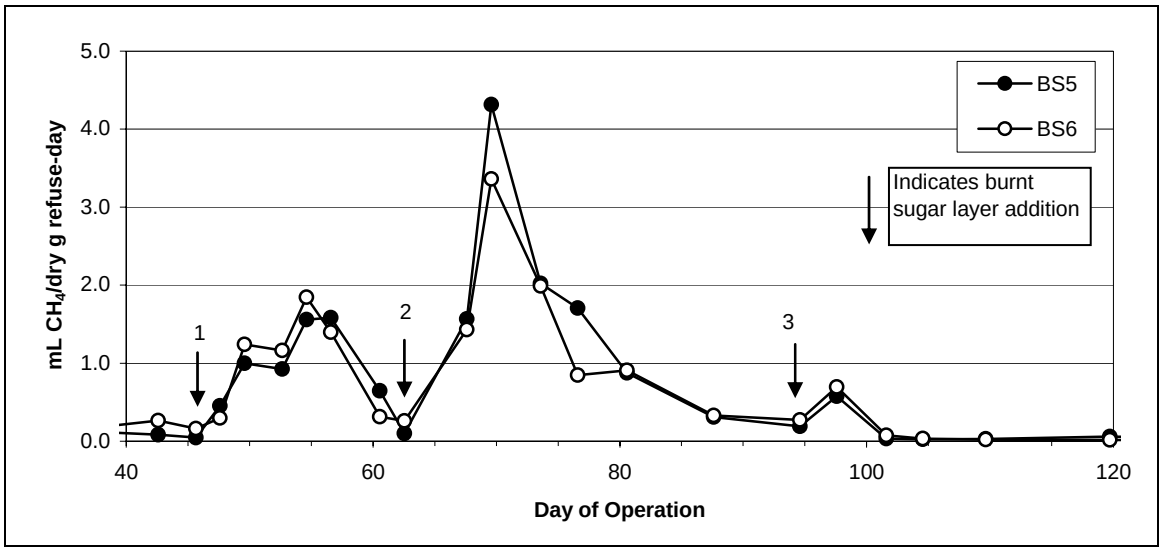

Figure 12: Methane production rates in reactors receiving burnt sugar layers. The numbers above the arrows refer to layer additions described in Table 4.

3.2.4 Discussion

With respect to the abiotic leaching experiment, the BS was shown to dissolve readily in the laboratory. However, under field conditions, the rate of dissolution will be influenced by ambient temperatures and the frequency and rate of infiltration. This may be beneficial as the material is released to the decomposing refuse more slowly.

The refuse system proved to be robust in degrading significantly more BS than was predicted on the basis of pH inhibition alone. As the BS additions increased in intensity, a COD accumulation and lengthening lag times for methane production were observed until the system failed at an addition of 295.1 g dissolved BS/g dry refuse. When the BS was added as a layer, failure occurred between 122 and 366 g BS/dry kg refuse. Apparently, the

rate of mixing of the layer into the refuse far exceeded the ability of the microorganisms to recover from the pH drop.

The results of this experiment define the maximum biodegradation capacity of decomposing refuse and provide a starting point for subsequent field experimentation. The results suggest that refuse in an active state of methane production can convert dissolved BS to methane without inhibition at BS additions up to 20% or 20 g BS/100 g dry refuse, or, for refuse at 20% moisture, 17 g BS/100 g of wet refuse. Under field conditions, the rate at which BS can be added will be governed as much by the temperature and the disposal method. The values developed from the laboratory work should be taken as upper limits. The results from these experiments suggest that the rate of methane production and the rate at which the system pH decreases are limited by the rate of mixing of BS into refuse. This implies that a thick layer of BS could be added to the surface of a landfill without significant inhibitory pH effects, but as the layer surface area increases, so do the rate of mixing and the potential for an inhibitory pH increase. All experimental work was conducted with refuse in an active state of methane production. It is important to note that fresh refuse cannot be expected to handle as much BS because microbial populations are not fully developed.

3.2.5 Conclusions

Overall conclusions of the burnt sugar research are presented below:

- The results suggest that actively decomposing refuse has the potential to attenuate relatively high loading of a highly degradable and low pH substrate.

- Actively-decomposing refuse can convert dissolved BS to methane without inhibition at additions up to 20% or 20 g BS/100 g dry refuse, or, for refuse at 20% moisture, 17 g BS/100 g of wet refuse.
- The refuse system degraded significantly more BS than was predicted on the basis of pH inhibition alone. As the BS additions increased in intensity, a COD accumulation, decreasing pH, increasing VFA levels, and lengthening lag times for methane production were observed until the system failed. The COD accumulation could be a result of a recalcitrant portion of the BS.
- High levels of propionic acid were observed immediately after BS additions. It is possible that there is a population of microorganisms present in the system that metabolizes lactic acid via a propionic acid pathway. Further research is planned to determine which species were present in the system.

3.3 Effect of Detergent Wastes on Refuse Decomposition

Detergent wastes are characterized in the first part of this section, followed by data on the ATAs and the refuse decomposition experiment.

3.3.1 Materials Characterization

The pH of the effluent softener and effluent soap were 3.4 and 6, respectively. The COD and TOC of the effluent soap were 141,100 mg/L and 19,740 mg/L, respectively. Although the surfactants in the wastes were unknown, research has shown that cationic surfactants are toxic to methanogens (Shcherbakova et al., 1999).

3.3.2 Anaerobic Toxicity Assays (ATAs)

ATAs were conducted at the following dilutions of detergent waste: 1%, 10%, 30%, and 50%. The tests were designed to determine the toxicity of the wastes and to determine whether they have methane potential above that of the ground refuse. Complete results are presented in Tables 8, 9, 10, and 11 below. For the effluent softener samples, the pH was neutralized using approximately 0.1 mL of 5M NaOH. This was done to ensure that pH was not a limiting factor in the toxicity assessment and BMP measurement. Gas production and composition analyses were performed on days 15 and 35 for the 10%, 30%, and 50% dilution experiments, and on day 14 for the 1% dilution.

The presence of either liquid waste inhibited methane production from ground refuse. Inhibition was complete at the 30 and 50% dilutions of the effluent softener. Inhibition was 67% at the 10% dilution. In the case of the effluent soap, inhibition was complete at the 10, 30 and 50% dilutions. There was zero potential for methane production in all dilutions tested for effluent soap and for 30% and 50% dilutions of effluent softener. A 10% dilution of effluent softener produced a low 1.4 mL CH_4/mL sample. Based on these results, tests were conducted at a 1% dilution. A 1% dilution of effluent softener did not exhibit inhibition and had a measurable methane potential. 1% dilutions of effluent soap exhibited 100% inhibition and produced no methane.

Table 8: Comparison of CH_4 yield from refuse in the presence and absence of liquid samples (10%, 30%, 50% dilutions)

Sample	Avg. mL CH_4 /gm[a]	Standard Deviation
Effluent Softener (10% + Refuse)	36.90	3.86
Effluent Softener (30% + Refuse)	-11.17	0.05
Effluent Softener (50% + Refuse)	-11.19	0.02
Effluent Soap (10% + Refuse)	-11.17	0.05
Effluent Soap (30% + Refuse)	-11.18	0.03
Effluent Soap (50% + Refuse)	-11.20	0.01
Refuse Blank	111.40	9.40

[a]Methane attributable to refuse after correction for background.

Table 9: Comparison of CH_4 yield of the liquid samples (10%, 30%, 50% dilutions)

Sample	Avg. mL CH_4/mL sample[a]	Standard Deviation
Effluent Softener (10%)	1.40	1.35
Effluent Softener (30%)	0.01	5.04
Effluent Softener (50%)	-0.11	0.00
Effluent Soap (10%)	-0.56	0.00
Effluent Soap (30%)	-0.19	0.00
Effluent Soap (50%)	-0.11	0.00
Inoculum Blank	5.61	0.21

[a]Methane attributable to refuse after correction for background

Table 10: Comparison of CH_4 yield from refuse in the presence and absence of liquid samples (1% dilution)

Sample	Avg. mL CH_4 /gm[a]	Standard Deviation
Effluent Softener (1% + Refuse)	101.97	8.24
Effluent Soap (1% + Refuse)	0.00	0.00
Refuse Blank	97.60	2.47

[a]Methane attributable to refuse after correction for background

Table 11: Comparison of CH_4 yield of the liquid samples (1% dilution)

Sample	Avg. mL CH_4/mL sample[a]	Stnd. Dev.
Effluent Softener (1%)	9.97	1.49
Effluent Softener (1%)	-4.36	0.08
Blank	5.56	0.76

[a]Methane attributable to refuse after correction for background

3.3.3 Refuse Decomposition Experiments

Refuse decomposition experiments were conducted to determine the maximum amounts of detergent wastes that could be added to an actively methanogenic system before inhibition. Methane production rates for the reactors are plotted in Figure 13. Additions of effluent softener up to 10.4% did not show significant inhibition in methane production. In fact, the methane potential of effluent softener gave higher methane production rates for reactors D4 to D6 than in the other reactors. The acidic pH of the wastes did not significantly affect the pH of reactor leachate, which remained neutral through all waste additions.

Leachate in reactors D7 to D9 was diluted on days 91 and 102 because it was hypothesized that too much waste had been added and that refuse decomposition was inhibited. The rate of decreasing methane production rate in reactors D7 to D9 after day 60 was steeper than in reactors D1 and D3, which supports this view. It was hypothesized that methane production in reactors D7 to D9 would increase after leachate dilution. However, it became necessary to add glucose solution to reactors D1, D2, and D7 to D9 at days 107 and 110 because it was difficult to resolve differences in methane production due to lack of degradable substrate. Table 12 presents the change in methane production rates after glucose

addition. The average rate change in reactors D7 to D9 was 33% that of D1 and D3, which gives evidence that there was inhibition at effluent soap concentrations of about 3%. The refuse decomposition experiments supported greater attenuation of detergent wastes than the ATA results. This could be due to increased likelihood for surface reactions in the refuse experiments than in the ATAs, which had a much lower solids to liquid ratio.

Table 12: Change in methane production rate after glucose additions at days 107 and 110. The rate change is the difference between the rate at day 112 and the rate at day 105.

Reactor	Effluent Soap %	Change in mL CH_4/dry g-d
D1	1.91	0.32
D3	1.93	0.40
D7	3.2	0.13
D8	3.25	0.15
D9	2.88	0.08

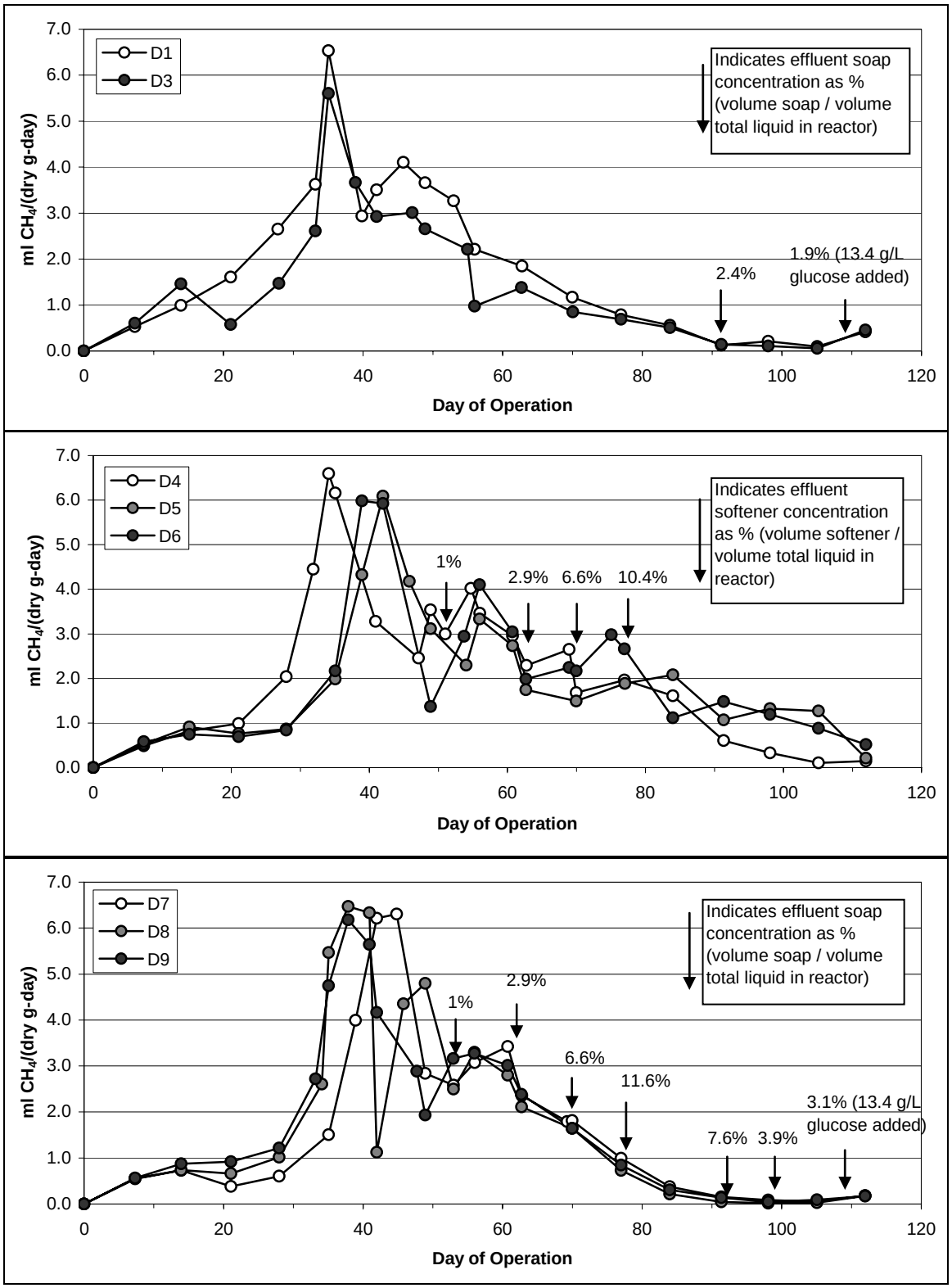

Figure 13: Methane production rates in the detergent reactors. Waste concentrations are expressed as an average percentage of volume of waste to volume of liquid in each set of reactors. Reactor D2 is excluded because it remained in the acid phase.

3.3.4 Conclusions

Overall conclusions of the detergent research are presented below:

- The ATAs demonstrated that even at a dilution of 1%, effluent soap completely inhibited methane production from refuse and had no methane production potential. A 1% dilution of effluent softener did not inhibit methane production, but 67% inhibition was observed at a 10% dilution of this waste.
- The refuse decomposition experiments demonstrated that effluent softener levels of 10% did not appear to inhibit methane production. There is evidence that methane production was inhibited at effluent soap concentrations of at least 3%.
- The refuse decomposition experiments support greater attenuation of the detergent wastes than the ATAs. This could be related to greater potential for surface reactions in the presence of solids.

4 REFERENCES

American Public Health Association., American Water Works Association., and Water Environment Federation. (1992). *Standard methods for the examination of water and wastewater*, 18th Ed., American Public Health Association, Washington, DC.

American Public Health Association., American Water Works Association., and Water Environment Federation. (1998). *Standard methods for the examination of water and wastewater*, 20th Ed., American Public Health Association, Washington, DC.

Barlaz, M. A., Ham, R. K., and Schaefer, D. M. (1990). "Methane Production From Municipal Refuse - A Review of Enhancement Techniques and Microbial Dynamics." *Critical Reviews in Environmental Control*, 19(6), 557-584.

Barlaz, M. A., Schaefer, D. M., and Ham, R. K. (1989). "Bacterial Population Development and Chemical Characteristics of Refuse Decomposition in a Simulated Sanitary Landfill." *Applied and Environmental Microbiology*, 55(1), 55-65.

Benson, C. H., Barlaz, M. A., Lane, D. T., and Rawe, J. M. (2007). "Practice review of five bioreactor/recirculation landfills." *Waste Management*, 27(1), 13-29.

Davis, M. W. (1998). "A rapid modified method for compositional carbohydrate analysis of lignocellulosics by high pH anion-exchange chromatography with pulsed amperometric detection (HPAEC/PAD)." *Journal of Wood Chemistry and Technology*, 18(2), 235-252.

Eleazer, W. E., Odle, W. S., Wang, Y. S., and Barlaz, M. A. (1997). "Biodegradability of municipal solid waste components in laboratory-scale landfills." *Environmental Science & Technology*, 31(3), 911-917.

Jjemba, P. K. (2004). *Environmental microbiology : principles and applications*, Science Publishers, Enfield, NH, USA.

Madigan, M. T., Martinko, J. M., and Parker, J. (2002). *Brock biology of microorganisms*, 10th Ed., Prentice Hall/Pearson Education, Upper Saddle River, NJ.

Martin, D. J., Potts, L. G. A., and Heslop, V. A. (2003). "Reaction mechanisms in solid-state anaerobic digestion - I. The reaction front hypothesis." *Process Safety and Environmental Protection*, 81(B3), 171-179.

McMahon, K. D., Stroot, P. G., Mackie, R. I., and Raskin, L. (2001). "Anaerobic codigestion of municipal solid waste and biosolids under various mixing conditions - II: Microbial population dynamics." *Water Research*, 35(7), 1817-1827.

Parkin, G. F., and Owen, W. F. (1986). "Fundamentals of Anaerobic-Digestion of Waste-Water Sludges." *Journal of Environmental Engineering-Asce*, 112(5), 867-920.

Pettersen, R. C., and Schwandt, V. H. (1991). "Wood Sugar Analysis by Anion Chromatography." *Journal of Wood Chemistry and Technology*, 11(4), 495-501.

Price, G. A., Barlaz, M. A., and Hater, G. R. (2003). "Nitrogen management in bioreactor landfills." *Waste Management*, 23(7), 675-688.

Reinhart, D. R., McCreanor, P. T., and Townsend, T. (2002). "The bioreactor landfill: Its status and future." *Waste Management & Research*, 20(2), 172-186.

Reynolds, C. S., and Davies, P. S. (2001). "Sources and bioavailability of phosphorus fractions in freshwaters: a British perspective." *Biological Reviews*, 76(1), 27-64.

Rhew, R. D., and Barlaz, M. A. (1995). "Effect of Lime-Stabilized Sludge as Landfill Cover on Refuse Decomposition." *Journal of Environmental Engineering-Asce*, 121(7), 499-506.

Rohrs, L. H., Fourie, A. B., and Blight, G. E. (1998). "Effects of sewage sludge and refuse composition on the rate of degradation and leachate quality of co-disposed waste in a water-deficient environment." *Water Sa*, 24(2), 137-146.

Shcherbakova, V.A., Laurinavichius, K.S. and Akimenko, V.K. (1999) Toxic effect of surfactants and probable products of their biodegradation on methanogenesis in an anaerobic microbial community. Chemosphere 39(11), 1861-1870.

Stroot, P. G., McMahon, K. D., Mackie, R. I., and Raskin, L. (2001). "Anaerobic codigestion of municipal solid waste and biosolids under various mixing conditions - I. Digester performance." *Water Research*, 35(7), 1804-1816.

Tchobanoglous, G.; Burton, F. L.; Metcalf & Eddy., *Wastewater engineering : treatment, disposal, and reuse*. 3rd ed.; McGraw-Hill: New York, 1991; p xvi, 1334 p.

Wang, Y. S., Byrd, C. S., and Barlaz, M. A. (1994). "Anaerobic Biodegradability of Cellulose and Hemicellulose in Excavated Refuse Samples Using a Biochemical Methane Potential Assay." *Journal of Industrial Microbiology*, 13(3), 147-153.

Zellner, G., Neudorfer, F., and Diekmann, H. (1994). "Degradation of Lactate by an Anaerobic Mixed Culture in a Fluidized-Bed Reactor." *Water Research*, 28(6), 1337-1340.

APPENDICES

Appendix A: Materials and Methods

Table A-1: Parts list for the refuse decomposition reactors used in the biosolids, burnt sugar, and detergent research

Function	Part Name	Part Number	Vendor
Reactor Ports for Air and Liquid Flow	Nalgene barbed bulkhead fitting kits, 1/4" tubing ID	EW-06259-10	Cole-Parmer
Gas Bag	Tedlar, 2 mil, 24"x 24" (44L) with foil (LAM) cover, and with two fittings at opposite corners of a diagonal—one JACO polypropylene tube fitting (JACOP) and one JACO polypropylene fitting with septum installed. Also: one Luer Valve (LUER) installed in LAM cover only, but on the opposite surface (NCOR)		Pollution Measurement Corporation
Reactor	2-gallon polypropylene mason jar	71169	United States Plastic Corp.
Gas Bag valve	1/4-28 polymer shut-off valve	P-721A	Upchurch Scientific
Tubing	Tygon lab tubing 1/4" ID x 3/8" OD, 50 ft/pack	EW-06408-50	Cole-Parmer
Tubing	Tygon lab tubing 3/16" ID x 5/16" OD, 50 ft/pack	EW-06408-03	Cole-Parmer
Leachate Bag	Empty all-in-one EVA container with connector (2000 mL)	68000-580 (Baxter 2B8122)	VWR Scientific
Tubing Clamps	Herbie clamps	AA, B, and BB	Speedy Products
Fitting from Tubing to Gas Bag	Chrome-plated brass male quick-turn x barb, for 1/4" To 5/16" tube ID	51465K117	McMaster-Carr
Gas Bag valve	Female luer to male threaded adapter	P-624	Upchurch Scientific
Reducing coupling	Nylon single barbed tube fitting reducing coupling for 1/4" X 3/16" tube ID	5463K152	McMaster-Carr
Tubing coupling	Nylon single-barbed tube fitting coupling for 1/4" tube ID	5463K578	McMaster-Carr
Gaskets	Silicone sealing washer 5/16" screw size, .290" ID, 11/16" OD, .093" thick	99604A119	McMaster-Carr
Tubing connector	Nylon single barbed tube fitting tee for 1/4" tube ID	5463K606	McMaster-Carr
Leachate Sampling Port	Nalgene single barbed tube fitting tee barb x male x barb for 1/4" tube ID, 1/8" NPT	5463K532	McMaster-Carr

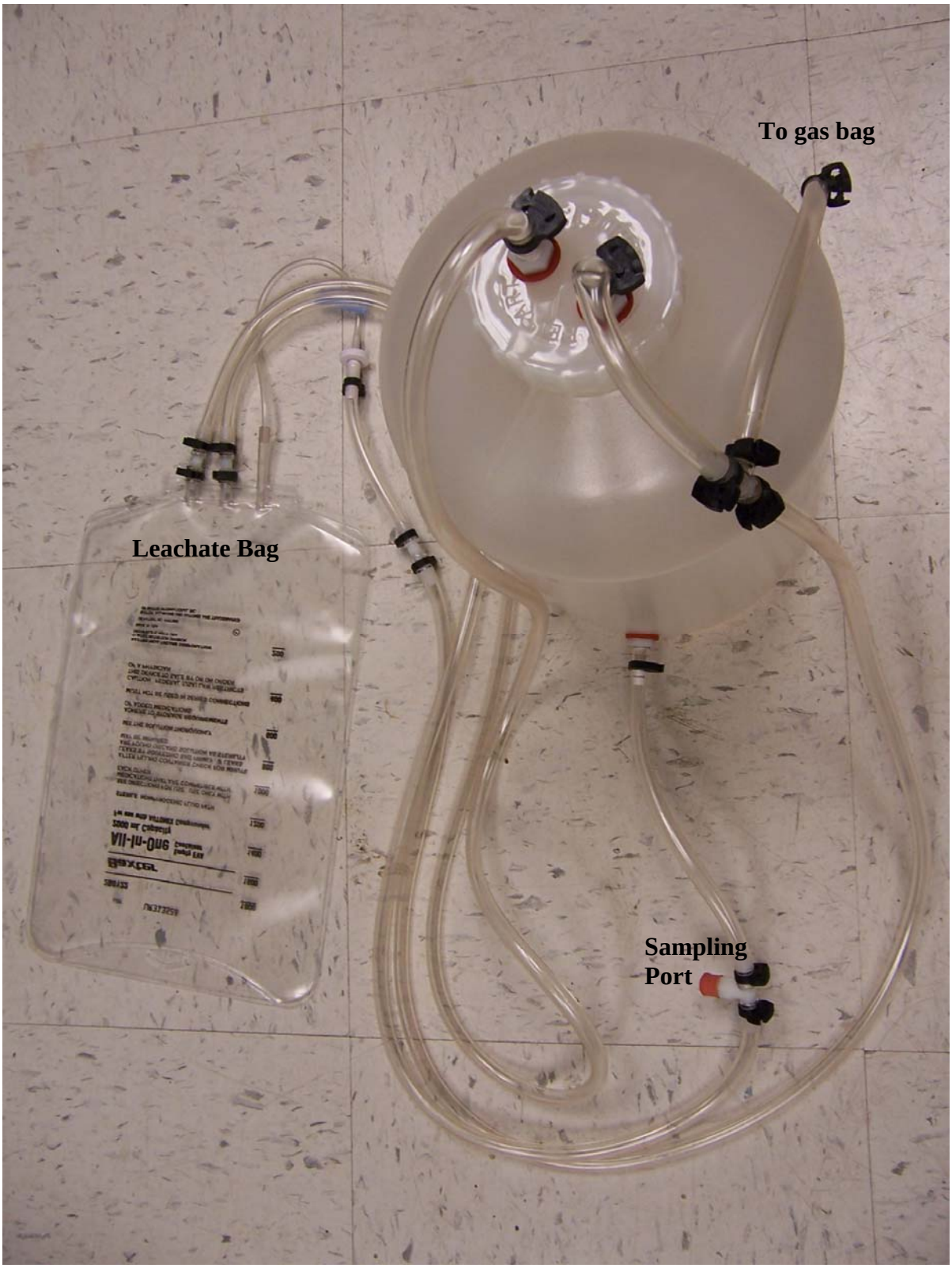

Figure A-1: Refuse decomposition reactor

Table A-2: Contents of each reactor.

Biosolids Reactors	Refuse Moisture Content (wet weight basis)	MSW (g wet weight)	MSW (g dry weight)	Biosolids Moisture Content (wet weight basis)	Biosolids (g wet weight)	Biosolids (g dry weight)	Total weight wet (g)	Total dry weight (g)
P1 (Biosolids Control)	28.9%	0.0	0.0	84.8%	1541.4	234.3	1541.4	234.3
P2 (Biosolids Control)	28.9%	0.0	0.0	84.8%	1694.1	257.5	1694.1	257.5
P3 (Refuse Control)	28.9%	2423.3	1723.0	84.8%	0.0	0.0	2423.3	1723.0
P4 (Refuse Control)	28.9%	2396.6	1704.0	84.8%	0.0	0.0	2396.6	1704.0
P5 (Refuse Control)	28.9%	2494.8	1773.8	84.8%	0.0	0.0	2494.8	1773.8
P6 (10% Biosolids)	28.9%	2551.2	1813.9	84.8%	255.1	38.8	2806.3	1852.7
P7 (10% Biosolids)	28.9%	2500.8	1778.1	84.8%	250.1	38.0	2750.9	1816.1
P8 (10% Biosolids)	28.9%	2614.3	1858.8	84.8%	261.4	39.7	2875.7	1898.5
P9 (20% Biosolids)	28.9%	2871.0	2041.3	84.8%	574.2	87.3	3445.2	2128.6
P10 (20% Biosolids)	28.9%	2778.7	1975.7	84.8%	555.7	84.5	3334.4	2060.1
P11 (20% Biosolids)	28.9%	2662.6	1893.1	84.8%	532.5	80.9	3195.1	1974.1

Burnt Sugar Reactors	Refuse MC (wet weight basis)	Refuse (wet weight)	Refuse (dry weight)
Control Population 1	58.9%	2004.3	823.8
Control Population 2	58.9%	2004.1	823.7
Control Methane Production 1 (BS1)	58.9%	2005.5	824.3
Control Methane Production 2 (BS2)	58.9%	1977.2	812.6
Acclimated Population 1	58.9%	2001.5	822.6
Acclimated Population 2	58.9%	2000.0	822.0
Acclimated Methane Production 1 (BS3)	58.9%	2005.6	824.3
Acclimated Methane Production 2 (BS4)	58.9%	2001.6	822.7
Non-Acclimated Population 1 (BS5)	58.9%	2003.5	823.4
Non-Acclimated Population 2	58.9%	2007.2	825.0
Non-Acclimated Methane Production 1 (BS6)	58.9%	2003.7	823.5
Non-Acclimated Methane Production 2	58.9%	2000.0	822.0

Detergent Reactors[a]	Fill Material Moisture Content (wet weight basis)	Fill Material (g wet weight)	Fill Material (g dry weight)[b]
D1 (Control)	43.3%	2450.7	1389.5
D2 (Control)	43.3%	2499.6	1417.3
D3 (Control)	43.3%	2450.4	1389.4
D4 (Blue Fabric Softener)	43.3%	2451.1	1389.8
D5 (Blue Fabric Softener)	43.3%	2450.3	1389.3
D6 (Blue Fabric Softener)	43.3%	2449.0	1388.6
D7 (Green Detergent)	43.3%	2447.0	1387.4
D8 (Green Detergent)	43.3%	2449.4	1388.8
D9 (Green Detergent)	43.3%	2450.0	1389.2

[a]Fill material consists of 25% office paper and 75% decomposing refuse (wet wt.). Office paper had no initial moisture.

[b]Fill material (dry g) = Fill material (wet g) * [1- (Fill material moisture content %/100)]

Table A-3: Schedules of major leachate removals and DI water additions to the biosolids reactors. Note that removal of leachate samples is not considered.

P3

Day	Water Added (mL)	Description	Leachate Removed (mL)
0	700	Moisture due to refuse	0
0	2500	Initial DI water addition	0
1	500	DI water addition	0
46	200	DI water addition	0
60	500	DI water addition	765
62	500	DI water addition	480
62	600	DI water addition	410
98	1000	DI water addition	690
101	2000	DI water addition	880
102	0		990
112	1000	Methanogenic Leachate	930

P4

Day	Water Added (mL)	Description	Leachate Removed (mL)
0	693	Moisture due to refuse	0
0	2500	Initial DI water addition	0
1	500	DI water addition	0
46	200	DI water addition	0
60	500	DI water addition	590
62	500	DI water addition	590
62	600	DI water addition	440
98	1000	DI water addition	810
101	1900	DI water addition	935
102	0		985
112	1000	Methanogenic Leachate	960

P5

Day	Water Added (mL)	Description	Leachate Removed (mL)
0	721	Moisture due to refuse	0
0	2000	Initial DI water addition	0
8	100	DI water addition	0
11	200	DI water addition	0
24	250	DI water addition	0
46	200	DI water addition	0
60	500	DI water addition	690
62	500	DI water addition	420
62	600	DI water addition	370
98	1000	DI water addition	715
101	2000	DI water addition	720
102	0		990
112	1000	Methanogenic Leachate	760

P6

Day	Water Added (mL)	Description	Leachate Removed (mL)
0	216	Moisture due to biosolids	0
0	954	Moisture due to refuse	0
0	2000	Initial DI water addition	0
1	500	DI water addition	0
29	200	DI water addition	0
46	200	DI water addition	0
60	500	DI water addition	565
62	500	DI water addition	500
62	600	DI water addition	405
98	1000	DI water addition	610
101	2000	DI water addition	980
102	0		1005
112	1000	Methanogenic Leachate	975

P7

Day	Water Added (mL)	Description	Leachate Removed (mL)
0	212	Moisture due to biosolids	0
0	723	Moisture due to refuse	0
0	2000	Initial DI water addition	0
1	500	DI water addition	0
25	100	DI water addition	50
46	200	DI water addition	0
60	500	DI water addition	730
62	500	DI water addition	470
62	600	DI water addition	350
98	1000	DI water addition	790
101	2000	DI water addition	925
102	0		995
112	1000	Methanogenic Leachate	810

P8

Day	Water Added (mL)	Description	Leachate Removed (mL)
0	222	Moisture due to biosolids	0
0	756	Moisture due to refuse	0
0	2000	Initial DI water addition	0
1	500	DI water addition	0
46	200	DI water addition	0
60	500	DI water addition	760
62	500	DI water addition	490
62	600	DI water addition	330
76	250	DI water addition	0
98	1000	DI water addition	1010
101	2000	DI water addition	1040
102	0		1000
112	1000	Methanogenic Leachate	820

P9

Day	Water Added (mL)	Description	Leachate Removed (mL)
0	487	Moisture due to biosolids	0
0	830	Moisture due to refuse	0
0	2000	Initial DI water addition	0
1	500	DI water addition	0
46	200	DI water addition	0
60	500	DI water addition	830
62	500	DI water addition	440
62	600	DI water addition	355
98	1000	DI water addition	710
101	1700	DI water addition	910
102	0		995
112	1000	Methanogenic Leachate	720

P10

Day	Water Added (mL)	Description	Leachate Removed (mL)
0	471	Moisture due to biosolids	0
0	803	Moisture due to refuse	0
0	2000	Initial DI water addition	0
1	500	DI water addition	0
46	200	DI water addition	0
60	500	DI water addition	490
62	500	DI water addition	490
62	600	DI water addition	470
98	1000	DI water addition	800
101	2000	DI water addition	930
102	0		1020
112	1000	Methanogenic Leachate	880

P11

Day	Water Added (mL)	Description	Leachate Removed (mL)
0	452	Moisture due to biosolids	0
0	769	Moisture due to refuse	0
0	2000	Initial DI water addition	0
1	500	DI water addition	0
46	200	DI water addition	0
60	500	DI water addition	660
62	500	DI water addition	435
62	600	DI water addition	425
74	250	DI water addition	0
98	1000	DI water addition	885
101	2000	DI water addition	955
102	0		975
112	1000	Methanogenic Leachate	750

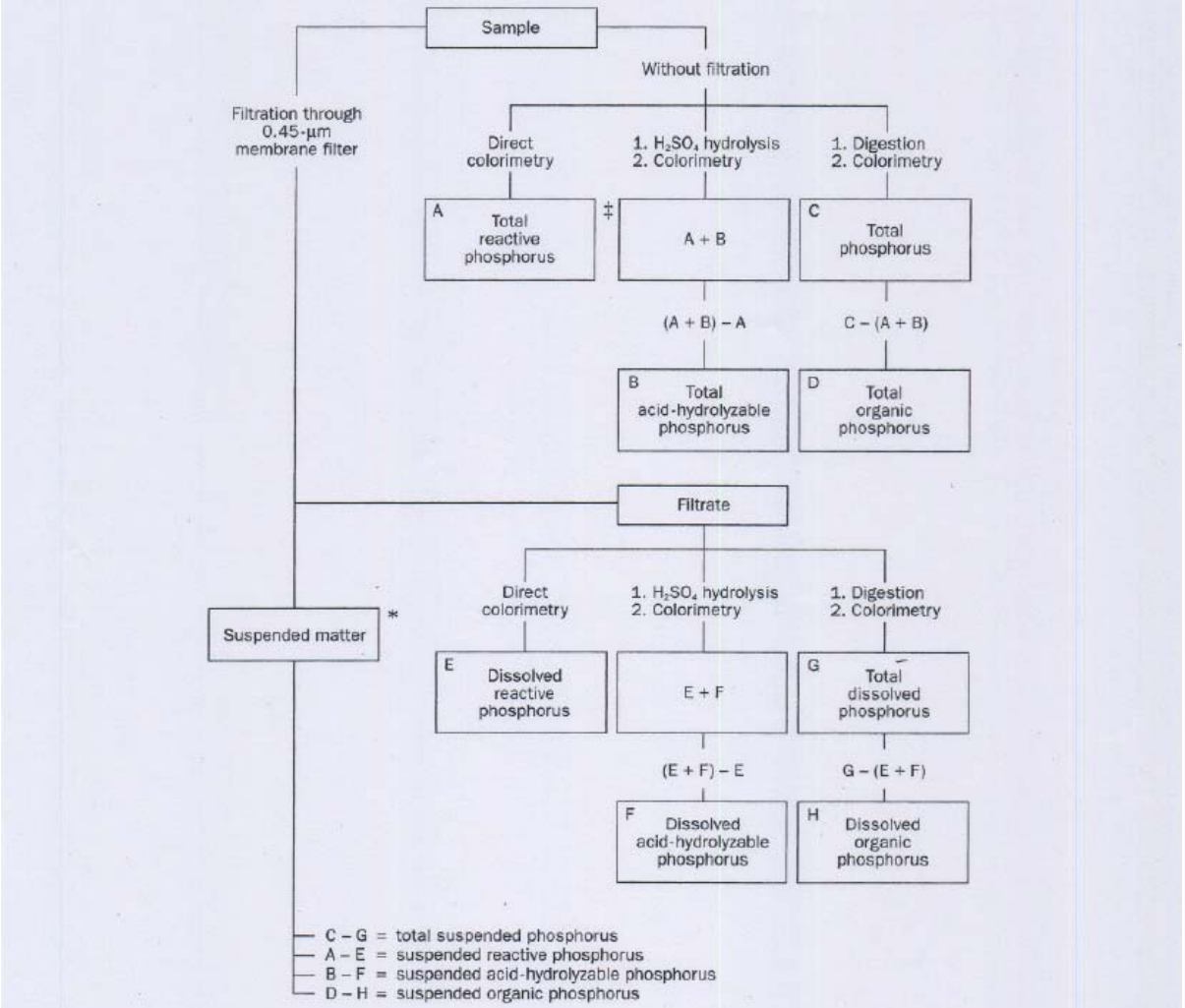

Figure 4500-P:1. Steps for analysis of phosphate fractions.

* Direct determination of phosphorus on the membrane filter containing suspended matter will be required where greater precision than that obtained by difference is desired. Digest filter with HNO_3 and follow by perchloric acid. Then perform colorimetry.
† Total phosphorus measurements on highly saline samples may be difficult because of precipitation of large quantities of salt as a result of digestion techniques that drastically reduce sample volume. For total phosphorus analyses on such samples, directly determine total dissolved phosphorus and total suspended phosphorus and add the results.
‡ In determination of total dissolved or total suspended reactive phosphorus, anomalous results may be obtained on samples containing large amounts of suspended sediments. Very often results depend largely on the degree of agitation and mixing to which samples are subjected during analysis because of a time-dependent desorption of orthophosphate from the suspended particles.

Figure A-2: Excerpt of flowchart for analysis of phosphate fractions from Standard Methods (APHA, 1998)

Preliminary work was conducted to measure the effect of oxidation on P and Fe concentrations and to verify a sampling strategy in which leachate samples were maintained under anaerobic conditions. The results are summarized in Table A-4. It was hypothesized that Fe would precipitate during aeration, PO_4 would sorb to $Fe(OH)_{3(s)}$, the precipitate would be filtered out, and that analysis of the filtrate would show lower P and Fe

concentrations than in a sample maintained under anaerobic conditions. However, at an Fe concentration of 15 mg/L, aqueous PO_4 losses under aerobic conditions were on the order of 10% based on limited testing.

Table A-4: Assessment of effect of aeration on measured phosphate concentrations. Samples were filtered and prepared for analysis as described in the Analytical Methods and Data Analysis section.

Analysis	Aerobic	Anaerobic	
30 minutes of aeration			
DRP	11.6	10.7	mg/L as PO_4
DHP	12.7	13.7	mg/L as PO_4
DTP	26.7	20.8	mg/L as PO_4
Fe (II)[1]	9.3	11.4	mg/L as Fe
Total Fe[1]	10.0	10.7	mg/L as Fe
22.5 hr of aeration			
DRP	42.0	47.6	mg/L as PO_4
DTP	48.8	52.3	mg/L as PO_4
Total Fe[2]	15.0	16.1	mg/L as Fe

[1]Standard Method 3500-FE D (APHA, 1998)
[2]Analyzed by ICP

Table A-5 presents the results of preliminary work to validate the methods used for the analysis of reactive, acid-hydroyzable, and organic phosphate. Known additions of potassium phosphate, sodium pyrophosphate, and adenosine monophosphate (AMP) were used to represent ortho-P, AHP, and organic P, respectively. As presented in Table A-5, the methods for DRP, DHP, and DTP were robust and were able to distinguish between different forms of PO_4.

Table A-5: Phosphorus Analytical Methods Validation

Objective	Result	Interpretation
The DRP of 5 mg/L pyro-P was measured	0.1 mg/L DRP	Very little pyro-P was recovered as DRP
The DHP of 0.8, 2.5, and 4.3 mg/L pyro-P were measured	0.8, 2.4, 4.1 mg/L DHP	The pyro-P was essentially all recovered as DHP
The DRP of 5 and 15.5 mg/L AMP were measured	0, 0 mg/L DRP	None of the AMP was recovered as DRP
The DHP of 5 mg/L AMP was measured	0.9, 0.9 mg/L DHP	18% of the AMP was recovered as DHP
The DTP of 0.8, 1.5, and 3.1 mg/L AMP were measured	0.7, 1.4, 2.8 mg/L DTP	90% of the AMP was recovered as DTP
The DRP of 0.5 and 3 mg/L ortho-P was measured before and after filtration through 0.45 µm nylon	Before: 0.49, 2.97 mg/L DRP After: 0.49, 2.97 mg/L DRP	Filtration has no effect on ortho-P recovered as DRP
The DHP of 1 mg/L pyro-P was measured before and after filtration through 0.45 µm nylon	Before: 0.9, 0.9 mg/L DHP After: 0.9, 0.9 mg/L DHP	Filtration has no effect on pyro-P recovered as DHP
The DTP of 0.5 and 2 mg/L AMP was measured before and after filtration through 0.45 µm nylon	Before: 0.5, 0.5, 1.8, 1.8 mg/L DTP After: 0.5, 0.5, 1.8, 1.8 mg/L DTP	Filtration has no effect on AMP recovered as DTP
The DRP of a solution of 1 mg/L ortho-P, 1 mg/L pyro-P, and 1 mg/L AMP was measured	1 mg/L DRP	The expected DRP was recovered
The DTP of a solution of 1 mg/L ortho-P, 1 mg/L pyro-P, and 1 mg/L AMP was measured	2.9 mg/L DTP	The expected DTP was recovered
The DHP of a solution of 1 mg/L ortho-P, 1 mg/L pyro-P, and 1 mg/L AMP was measured	2 mg/L DHP	The expected DHP was recovered
The DRP of a solution of 1 mg/L ortho-P, 1 mg/L pyro-P, and 1 mg/L AMP spiked with anaerobic MSW leachate containing 2.1 mg/L DRP was measured	3.2 mg/L DRP	The expected DRP was recovered
The DRP of a solution of 0.5 mg/L ortho-P, 0.5 mg/L pyro-P, and 0.5 mg/L AMP spiked with anaerobic MSW leachate containing 1.1 mg/L DRP was measured	1.6 mg/L DRP	The expected DRP was recovered
The DTP of solutions of 0.5 mg/L ortho-P, 0.5 mg/L pyro-P, and 0.5 mg/L AMP spiked with anaerobic MSW leachate containing 0.4 mg/L DTP were measured	1.9, 1.9, 1.8 mg/L DTP	The expected DTP was recovered
The DHP of solutions of 0.5 mg/L ortho-P, 0.5 mg/L pyro-P, and 0.5 mg/L AMP spiked with anaerobic MSW leachate containing 1.4 mg/L DHP were measured	2.3, 2.3, 2.4 mg/L DHP	The expected DHP was recovered

Note: All concentrations are reported as PO_4
ortho-P: potassium phosphate
pyro-P: sodium pyrophosphate
AMP: adenosine monophosphate

Table A-6: ICP results from the University of Georgia Chemical Analysis Laboratory for the composite dried ground biosolids and refuse samples used to fill the biosolids reactors.

Element	Biosolids (ppm)	Refuse (ppm)
Al	7123	8218
B	26.53	22.55
Ba	545.5	49.66
Ca	7875	13380
Cd	6.507	2.244
Co	5.205	2.505
Cr	13.62	12.3
Cu	198.4	28.3
Fe	15030	2487
K	1083	1740
Mg	1111	728.7
Mn	373.6	148.4
Na	373.7	1709
Ni	10.93	6.033
P	15830	2497
Pb	5.317	3.213
Si	1583	9638
Sr	186.1	34.52
Zn	554.6	236.1
As	0.9626	0.9349

Table A-7 presents the results of the glycosyl composition analysis performed by the University of Georgia Complex Carbohydrate Research Center on a burnt sugar sample. The analysis was performed by gas chromatography/mass spectrometry (GC/MS) of the per-*O*-trimethylsilyl (TMS) derivatives of the monosaccharide methyl glycosides produced from the sample by acidic methanolysis. The beginning sample provided to the laboratory contained 1 mg BS/mL. Methyl glycosides were first prepared from burnt sugar solution. 1 mL of sample and 20ul of a 1mg/ml solution of inositol were lyophilized together and analyzed by methanolysis in 1 M HCl in methanol at 80°C (18-22 hours), followed by re-*N*-acetylation with pyridine and acetic anhydride in methanol (for detection of amino sugars). The samples were then per-*O*-trimethylsilylated by treatment with Tri-Sil (Pierce) at 80°C (0.5 hours). [These procedures were carried out as previously described in Merkle and Poppe (1994) *Methods Enzymol*. 230: 1-15; York, et al. (1985) *Methods Enzymol.* 118:3-40.] GC/MS analysis of the TMS methyl glycosides was performed on an HP 5890 GC interfaced to a 5970 MSD, using an All Tech EC-1 fused silica capillary column (30m × 0.25 mm ID). From the 1 mL sample lyophilized, 750 μg from the expected 1000 μg was recovered. Further testing revealed the possibility that lactic acid volatilization was responsible for the incomplete recovery. Therefore, although the values given by the laboratory were on a 750 μg basis, the values were adjusted to reflect a 1000 μg basis.

Table A-7: Glycosyl Composition Analysis on Burnt Sugar Sample

Glycosyl Residue	Mass (µg)	Mole %[1]	% of BS
Ribose (Rib)	n.d.	n.d.	
Rhamnose (Rha)	8.4	5.4	0.8
Fucose (Fuc)	7.6	4.9	0.8
Xylose (Xyl)	n.d.	n.d.	
Glucuronic Acid	5.6	3.1	0.6
Galacturonic acid	n.d.	n.d.	
Mannose (Man)	n.d.	n.d.	
Galactose (Gal)	12.7	7.5	1.3
Glucose (Glc)	121.9	71.5	12.2
N Acetyl Galactosamine	n.d.	n.d.	
N Acetyl Glucosamine	16.0	7.6	1.6
Heptose(Hep)	n.d.	n.d.	
3 Deoxy-2-manno-2 Octulsonic acid	n.d.	n.d.	
Sum	**172.2**	**100.00**	

[1]Values are expressed as mole percent of total carbohydrate.
n.d.= none detected

Glucose % of BS calculation: 121.9 µg glucose / 1000 µg BS = **12.2% glucose**

Table A-8 presents a lactic acid analysis performed on a burnt sugar sample. The results are reported as g lactic acid/g burnt sugar.

Table A-8: Lactic acid analysis on sample of burnt sugar.

Date Analyzed: 4/11/06 DCB7/45

Standard Curve Information:

Lower Quantitation Limit	10 mg/L
Upper Quantitation Limit	100 mg/L

0.985 gms lactic acid diluted to 1L DI water = 97.4 mg/l as lactate
Prepared a 10, 50, and 100 mg/L standard curve.

Sample Information:

Sample ID	Dilution X	Lactate mg/L	gms/L burnt sugar	gm lactate/ gm burnt sugar	gm lactic acid gm burnt sugar
Run 1	25	1,010.8	1.4	0.722	0.730
Run 2	25	1,006.7	1.4	0.719	0.727

AS11-HC column
1.0 ml/min flow
137 mA suppressor current
30C oven

Eluent Generator Gradient
5 mM and hold for 6 minutes
Flush at 55 mM for 3 minutes then back to 5 mM

Table A-9: Analysis of burnt sugar COD by component. Grams of component over gram burnt sugar values are calculated from Table A-7 and Table A-8.

Component	**Chemical Formula**	**Molar Mass**	**g Component/ g BS**	**Moles O_2/ Mole Component**	**mg COD/g BS due to component**
Lactic Acid	$C_3H_6O_3$	90	0.730	3.0	779
Glucose	$C_6H_{12}O_6$	180	0.122	6.0	130
N Acetyl Glucosamine	$C_8H_{15}NO_6$	221	0.016	8.0	19
Galactose	$C_6H_{12}O_6$	180	0.013	6.0	14
Rhamnose	$C_6H_{12}O_5$	164	0.008	6.5	10
Fucose	$C_6H_{12}O_5$	164	0.008	6.5	10
Glucuronic Acid	$C_6H_{10}O_7$	194	0.006	5.0	5
Sum of Components	**-**	**-**	**0.903**	**-**	**966**
Burnt Sugar	**-**	**-**	**1.000**	**-**	**1230**
Percent of burnt sugar COD explained by COD of components:					79%

Appendix B: Results

Biosolids Results

Table B-1 presents the lag times to methanogenesis in the P reactors. Lag time is defined as the amount of time until the beginning of a steady increase in methane production rate which culminates in the peak methane production rate. A significant difference between the average means of the lag times among the treatments was not observed.

Table B-1: Lag times to methanogenesis in reactors P3 to P11. P5 did not reach methanogenesis.

Reactor	Treatment	Lag time (d)
P3	Refuse Control	131
P4	Refuse Control	145
P6	10% Biosolids	178
P7	10% Biosolids	157
P8	10% Biosolids	67
P9	20% Biosolids	67
P10	20% Biosolids	67
P11	20% Biosolids	157

Table B-2: DRP, DHP, and DTP in the P Reactors

Reactor	Day of Operation	DRP	DHP	DTP
P1	12	233.2		
P1	19	271.7	230.2	361.1
P1	26	305.6		
P1	33	328.3		
P1	40	343.4		332.8
P1	61	347.3		
P1	71	359.0		
P1	84	359.0	513.9	403.4
P1	98	406.2		
P1	109	382.7		
P1	126	387.4		
P2	12	233.2		
P2	19	267.9	273.1	332.8
P2	26	328.3		
P2	33	335.8		
P2	40	343.4	391.0	375.2

Reactor	Day of Operation	DRP	DHP	DTP
P2	61	359.0		
P2	71	382.4		
P2	84	405.8	374.9	459.9
P2	98	423.8		
P2	109	412.0		
P2	126	416.8		
P3	25	76.1		
P3	32	117.0		
P3	39	111.0		
P3	53	117.0		
P3	60	110.7		
P3	74	43.1		62.9
P3	84	51.5		
P3	97	218.6		234.0
P3	111	95.7		
P3	122	110.4		
P3	139	69.0		
P3	159	2.7		7.4
P3	181	16.0		
P3	227	31.7		
P3	263	42.8		
P4	25	93.0		
P4	32	56.6		
P4	39	70.2		
P4	53	53.6		
P4	60	56.6		
P4	74	12.7		23.7
P4	84	17.4		
P4	97	22.9		
P4	111	80.9	65.3	104.9
P4	122	79.5		
P4	139	25.0		
P4	159	11.8		
P4	181	1.0		4.6
P4	207	10.0		
P4	227	21.4		
P4	263	35.4		
P5	25	14.2	36.0	65.4
P5	32	17.0		
P5	39	14.7		
P5	53	24.5		
P5	60	31.8		
P5	74	44.1		
P5	84	30.3		
P5	97	81.4		
P5	111	94.2		
P5	122	125.0		148.8

Reactor	Day of Operation	DRP	DHP	DTP
P5	139	88.1		
P5	159	110.1		
P5	181	71.9		93.6
P5	207	67.9		
P5	227	53.8		
P5	263	45.8		
P6	25	12.3		50.5
P6	32	20.8		
P6	39	58.5		
P6	53	38.9		
P6	60	57.4		
P6	74	65.4		
P6	84	11.2		24.4
P6	97	17.8		
P6	111	90.4		
P6	122	185.3		
P6	139	94.2		
P6	159	123.5		
P6	181	53.2		40.3
P6	207	33.9		
P6	227	14.8		
P6	263	31.0		
P7	25	67.2		116.2
P7	32	97.4		
P7	39	104.9		
P7	53	88.3		
P7	60	104.8		
P7	74	154.2		
P7	84	58.8		
P7	97	199.4		201.7
P7	111	94.8		
P7	122	135.9		
P7	139	88.4		
P7	159	100.5		
P7	181	13.2		
P7	207	31.0		
P7	227	56.0		
P7	263	38.4		
P8	17			152.2
P8	25	221.8		238.2
P8	32	94.2		142.6
P8	39	141.2		163.1
P8	53	123.0	125.6	163.1
P8	60	142.8		176.8
P8	74	31.7		39.8
P8	84	22.2		39.8
P8	97	19.6		26.1

Reactor	Day of Operation	DRP	DHP	DTP
P8	111	7.4		26.1
P8	122	7.7		12.4
P8	139	13.2		26.1
P8	159	11.0		12.4
P8	181	14.3		19.2
P8	207	16.2		19.2
P8	227	19.9		26.1
P9	17			137.9
P9	25	225.8		252.5
P9	32	124.4		163.1
P9	39	79.2	104.1	111.7
P9	53	64.9		94.6
P9	60	107.7	93.4	149.4
P9	74	50.7		53.5
P9	84	42.7		43.2
P9	97	30.3		53.5
P9	111	11.1		26.1
P9	122	10.0		19.2
P9	139	16.4		26.1
P9	159	21.3		26.1
P9	181	36.7		39.8
P9	207	36.9		46.6
P9	227	42.0		46.6
P9	263	48.7		
P10	25	174.7	136.3	215.8
P10	32	116.9		
P10	39	62.6		
P10	53	50.6		78.5
P10	60	69.8		
P10	74	65.4		
P10	84	69.7		
P10	97	206.8		
P10	111	177.1		
P10	122	159.4		
P10	139	88.4		
P10	159	8.1		13.8
P10	181	22.9		
P10	207	28.0		
P10	227	47.9		
P10	263	76.7		
P11	25	104.0		
P11	32	29.4		
P11	39	18.9		
P11	53	10.2	34.6	39.9
P11	60	21.8		
P11	74	119.1		
P11	84	271.3		276.3

Reactor	Day of Operation	DRP	DHP	DTP
P11	97	148.4		
P11	111	65.4		
P11	122	124.2		
P11	139	94.2		
P11	159	68.2		
P11	181	22.8		30.5
P11	207	22.9		
P11	227	41.3		
P11	263	66.4		

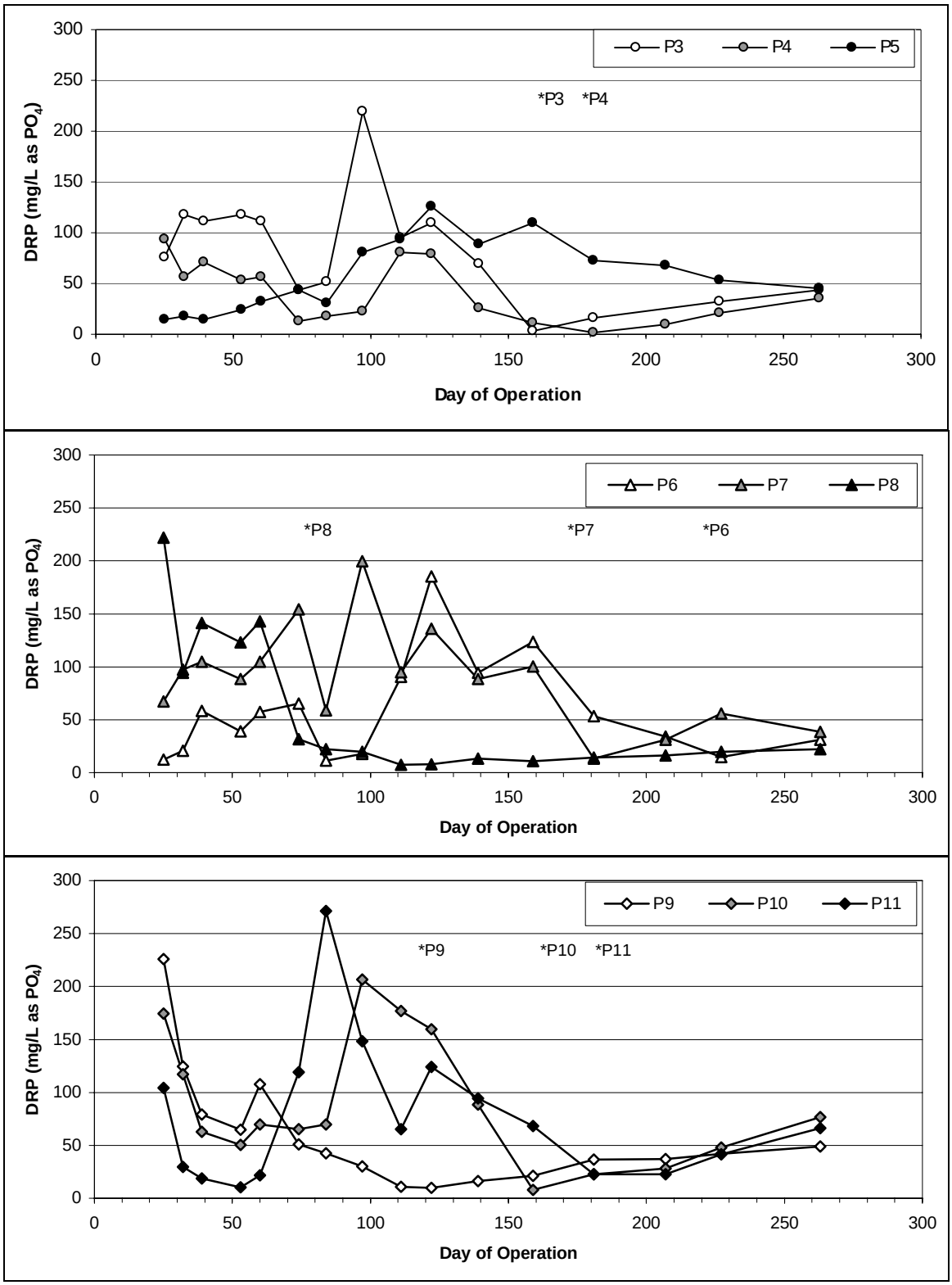

Figure B-1: DRP in reactors P3-P11, divided by treatment. The * followed by the reactor name denotes the day when the maximum methane production rate was measured in that reactor.

Table B-3: Leachate parameter correlation matrices (r) for reactors P3 to P11. The matrices were generated in StatCrunch.

Correlation matrix for Reactor = P3:

	pH (before neutr)	NH_4 (mg N/L)	Ca (mg/L)	Fe (mg/L)	Mg (mg/L)
NH_4 (mg N/L)	-0.65				
Ca (mg/L)	-0.90	0.86			
Fe (mg/L)	-0.58	-0.13	0.36		
Mg (mg/L)	-0.73	0.98	0.91	-0.03	
Reactive P (mg/L as PO_4)	-0.82	0.72	0.89	0.45	0.75

Correlation matrix for Reactor = P4:

	pH (before neutr)	NH_4 (mg N/L)	Ca (mg/L)	Fe (mg/L)	Mg (mg/L)
NH_4 (mg N/L)	-0.48				
Ca (mg/L)	-0.85	0.80			
Fe (mg/L)	-0.56	-0.33	0.11		
Mg (mg/L)	-0.69	0.92	0.95	-0.13	
Reactive P (mg/L as PO_4)	-0.58	0.45	0.74	0.02	0.63

Correlation matrix for Reactor = P5:

	pH (before neutr)	NH_4 (mg N/L)	Ca (mg/L)	Fe (mg/L)	Mg (mg/L)
NH_4 (mg N/L)	0.87				
Ca (mg/L)	0.83	0.80			
Fe (mg/L)	-0.69	-0.76	-0.41		
Mg (mg/L)	0.92	0.96	0.92	-0.66	
Reactive P (mg/L as PO_4)	-0.89	-0.78	-0.60	0.90	-0.78

Correlation matrix for Reactor = P6:

	pH (before neutr)	NH_4 (mg N/L)	Ca (mg/L)	Fe (mg/L)	Mg (mg/L)
NH_4 (mg N/L)	-0.00				
Ca (mg/L)	-0.87	0.23			
Fe (mg/L)	-0.76	-0.51	0.66		
Mg (mg/L)	-0.15	0.94	0.48	-0.29	
Reactive P (mg/L as PO_4)	-0.65	-0.26	0.52	0.64	-0.17

Correlation matrix for Reactor = P7:

	pH (before neutr)	NH_4 (mg N/L)	Ca (mg/L)	Fe (mg/L)	Mg (mg/L)
NH_4 (mg N/L)	-0.49				
Ca (mg/L)	-0.69	0.93			
Fe (mg/L)	-0.65	0.67	0.84		
Mg (mg/L)	-0.53	0.97	0.97	0.77	
Reactive P (mg/L as PO_4)	-0.76	0.35	0.61	0.75	0.44

Correlation matrix for Reactor = P8:

	pH (before neutr)	NH_4 (mg N/L)	Ca (mg/L)	Fe (mg/L)	Mg (mg/L)
NH_4 (mg N/L)	-0.81				
Ca (mg/L)	-0.93	0.58			
Fe (mg/L)	-0.98	0.79	0.90		
Mg (mg/L)	-0.98	0.88	0.88	0.95	
Reactive P (mg/L as PO_4)	-0.96	0.86	0.86	0.98	0.96

Correlation matrix for Reactor = P9:

	pH (before neutr)	NH_4 (mg N/L)	Ca (mg/L)	Fe (mg/L)	Mg (mg/L)
NH_4 (mg N/L)	-0.70				
Ca (mg/L)	-0.96	0.54			
Fe (mg/L)	-0.90	0.62	0.88		
Mg (mg/L)	-0.96	0.81	0.93	0.86	
Reactive P (mg/L as PO_4)	-0.78	0.56	0.73	0.92	0.74

Correlation matrix for Reactor = P10:

	pH (before neutr)	NH_4 (mg N/L)	Ca (mg/L)	Fe (mg/L)	Mg (mg/L)
NH_4 (mg N/L)	-0.61				
Ca (mg/L)	-0.96	0.66			
Fe (mg/L)	-0.92	0.49	0.94		
Mg (mg/L)	-0.77	0.93	0.82	0.70	
Reactive P (mg/L as PO_4)	-0.71	0.25	0.70	0.87	0.41

Correlation matrix for Reactor = P11:

	pH (before neutr)	NH_4 (mg N/L)	Ca (mg/L)	Fe (mg/L)	Mg (mg/L)
NH_4 (mg N/L)	-0.43				
Ca (mg/L)	-0.90	0.74			
Fe (mg/L)	-0.89	0.29	0.83		
Mg (mg/L)	-0.60	0.93	0.86	0.50	
Reactive P (mg/L as PO_4)	-0.66	-0.10	0.49	0.87	0.06

Figure B-2 presents a scatter plot of DRP vs. methane production rate at pH≥7 in the P reactors. A parallel analysis in which the DRP (C) was normalized with respect to the lowest measured DRP (C_o) did not improve the correlation (data not shown). One explanation is that leachate samples were not frequently collected and analyzed for DRP during maximum methane production and the true lowest DRP concentrations could have been missed.

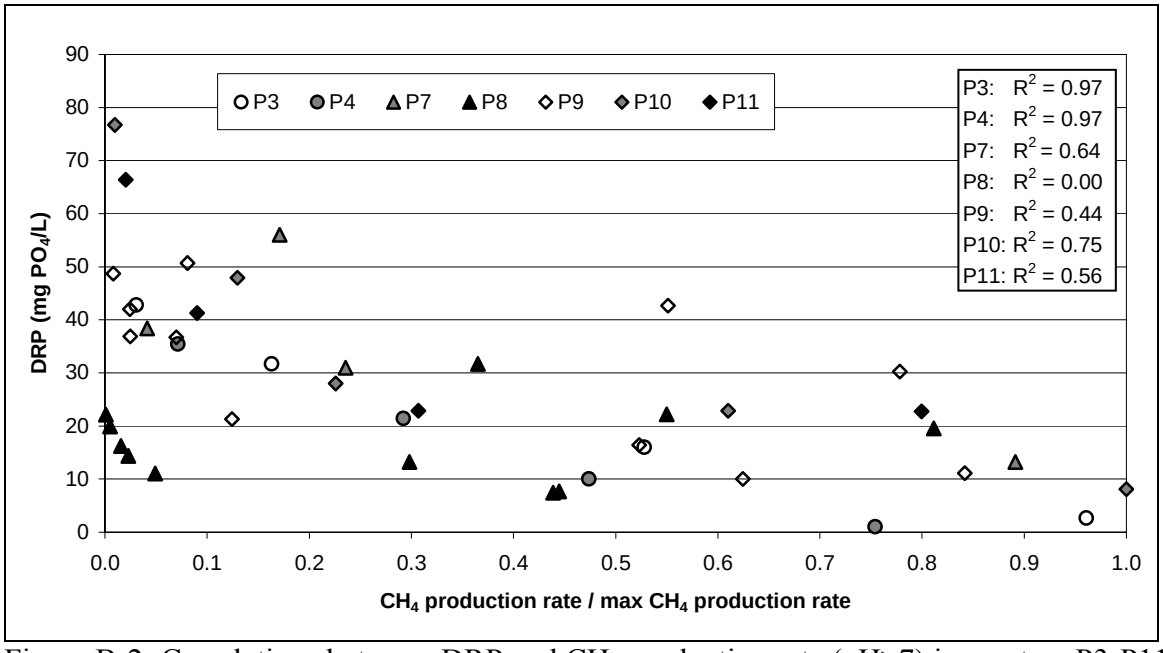

Figure B-2: Correlations between DRP and CH_4 production rate (pH≥7) in reactors P3-P11. P5 and P6 are omitted due to lack of sufficient data for a linear regression.

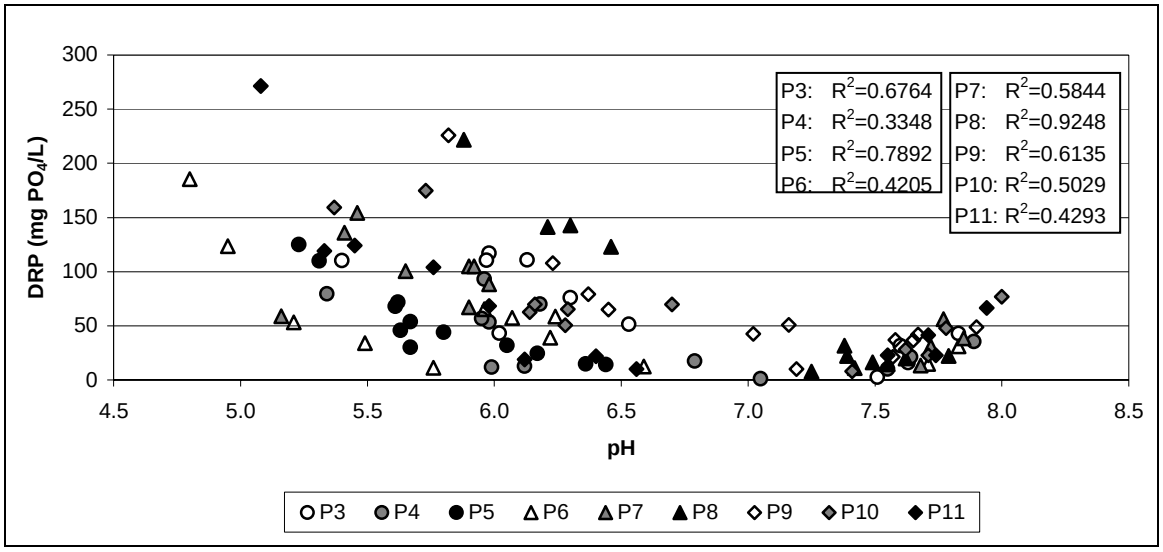

Figure B-3: Correlation between pH and DRP in reactors P3 to P11.

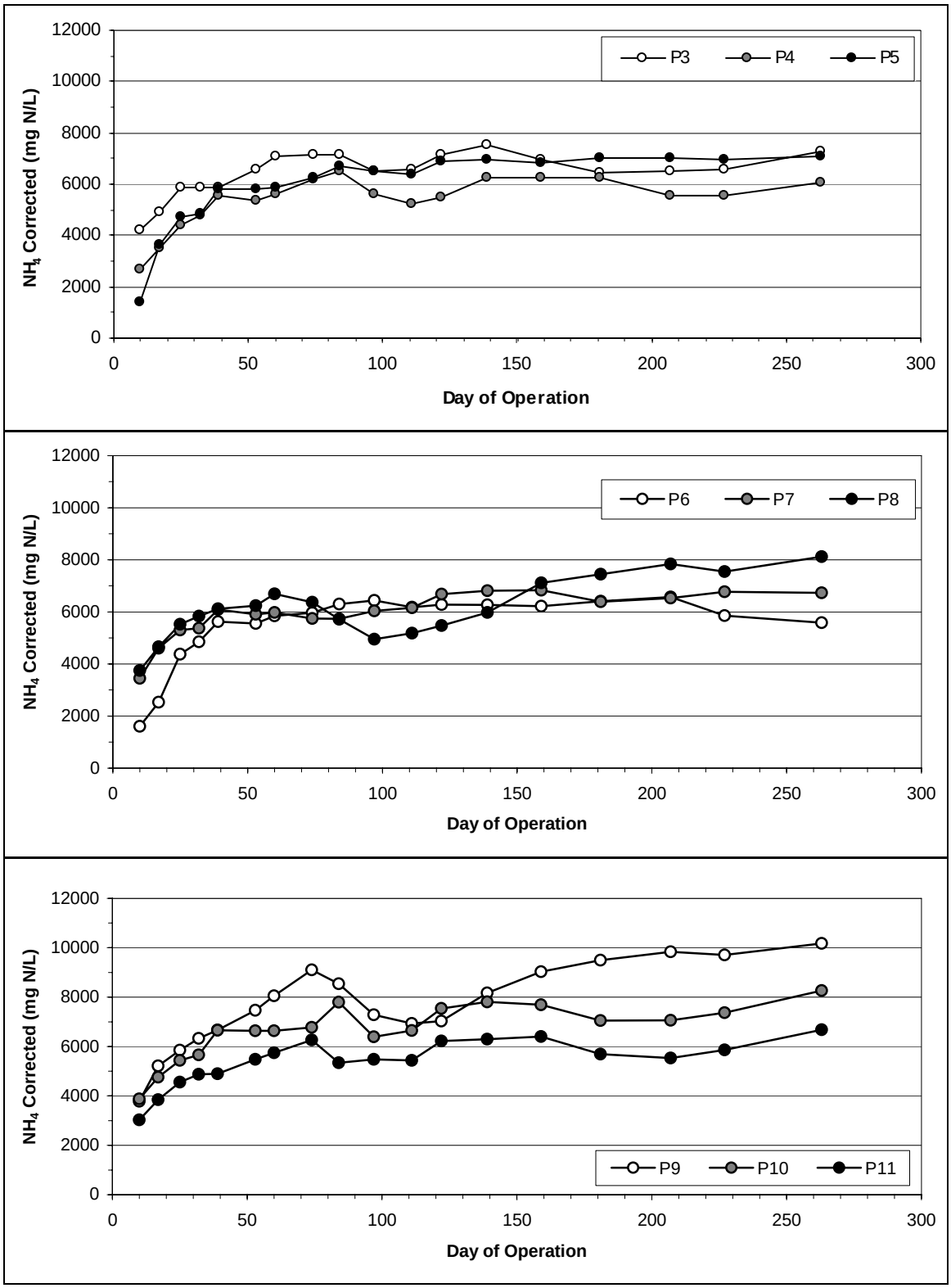

Figure B-4: Ammonia concentrations in the biosolids reactors. The concentration profiles are corrected for dilution (see Table A-3 for a schedule of leachate removals and DI water additions).

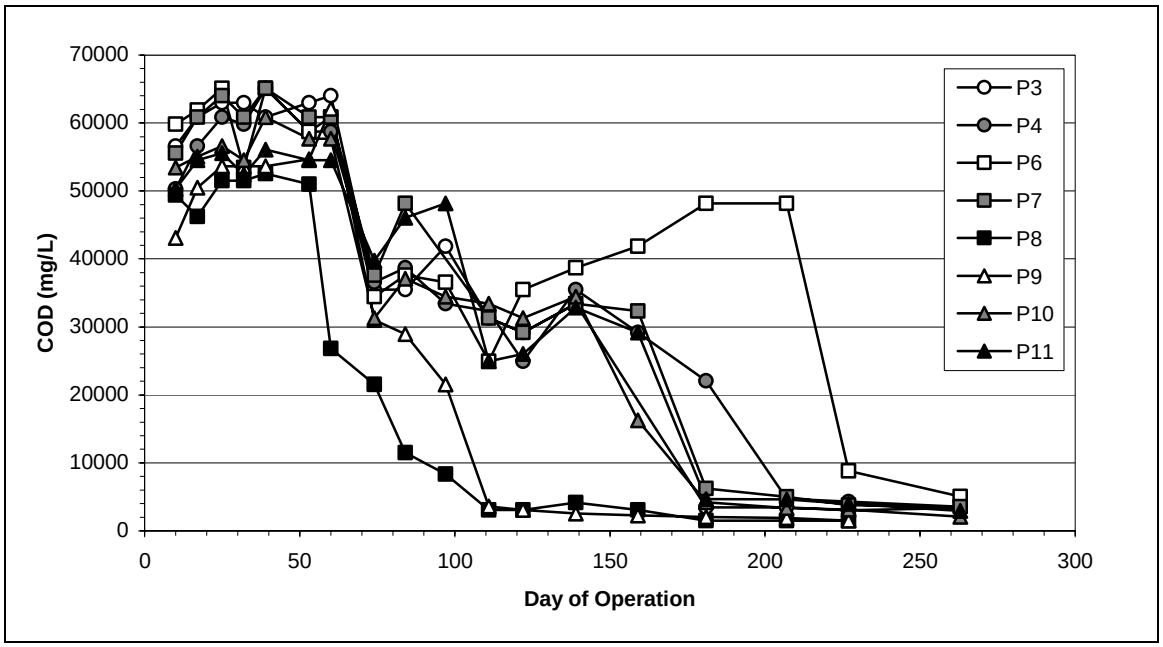

Figure B-5: COD concentrations in the biosolids reactors. P5 is excluded because it never neutralized.

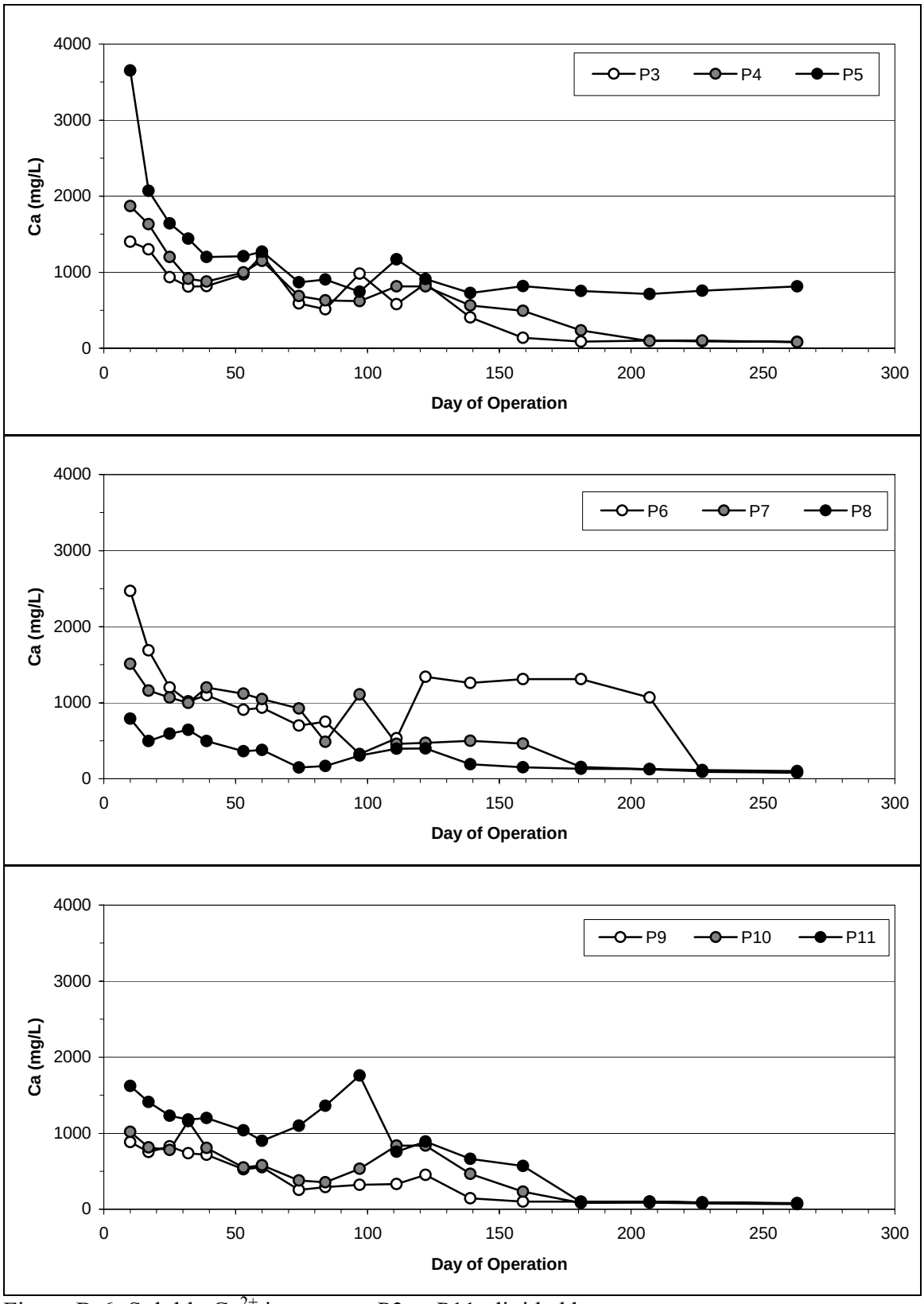

Figure B-6: Soluble Ca^{2+} in reactors P3 to P11, divided by treatment.

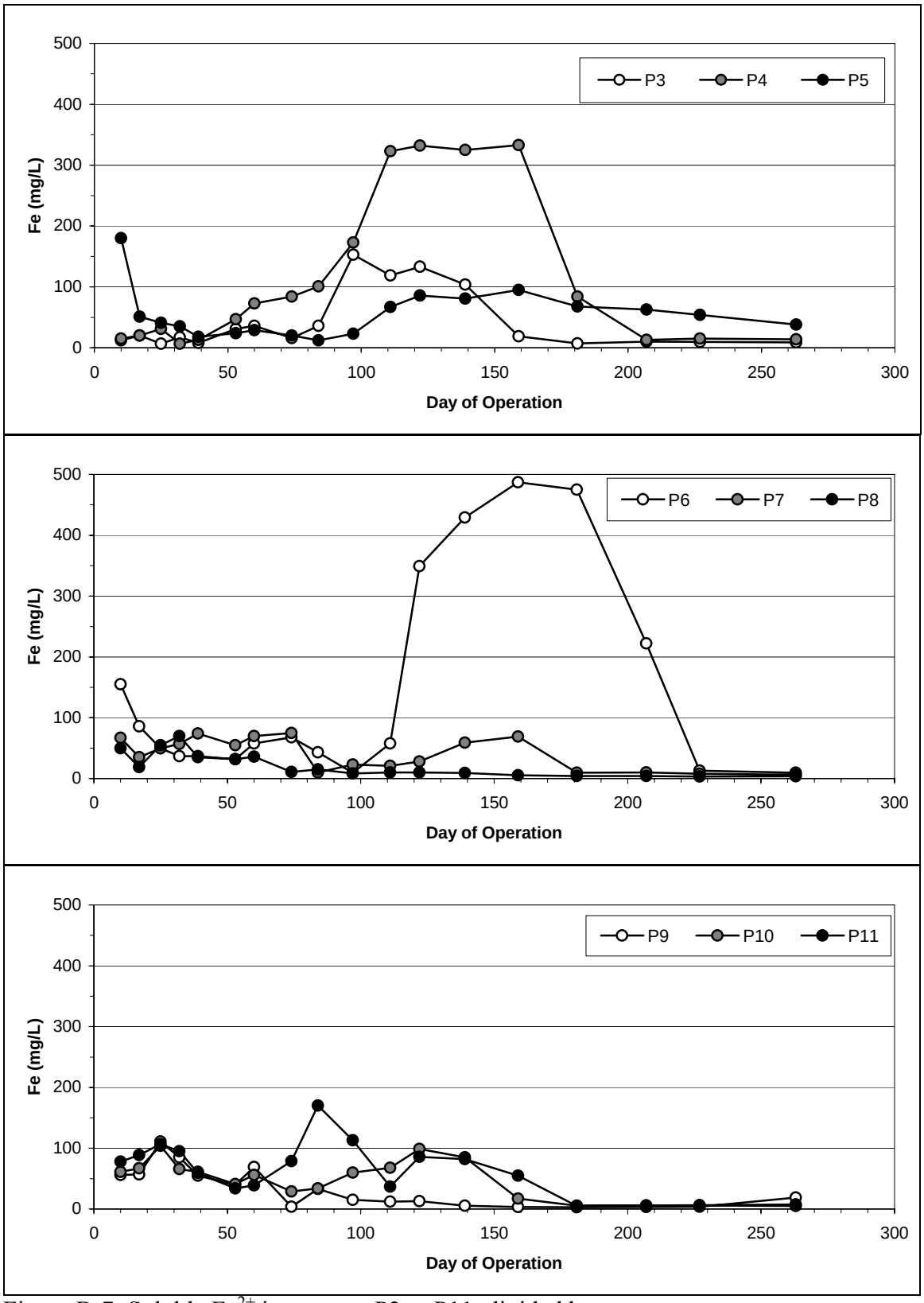

Figure B-7: Soluble Fe^{2+} in reactors P3 to P11, divided by treatment.

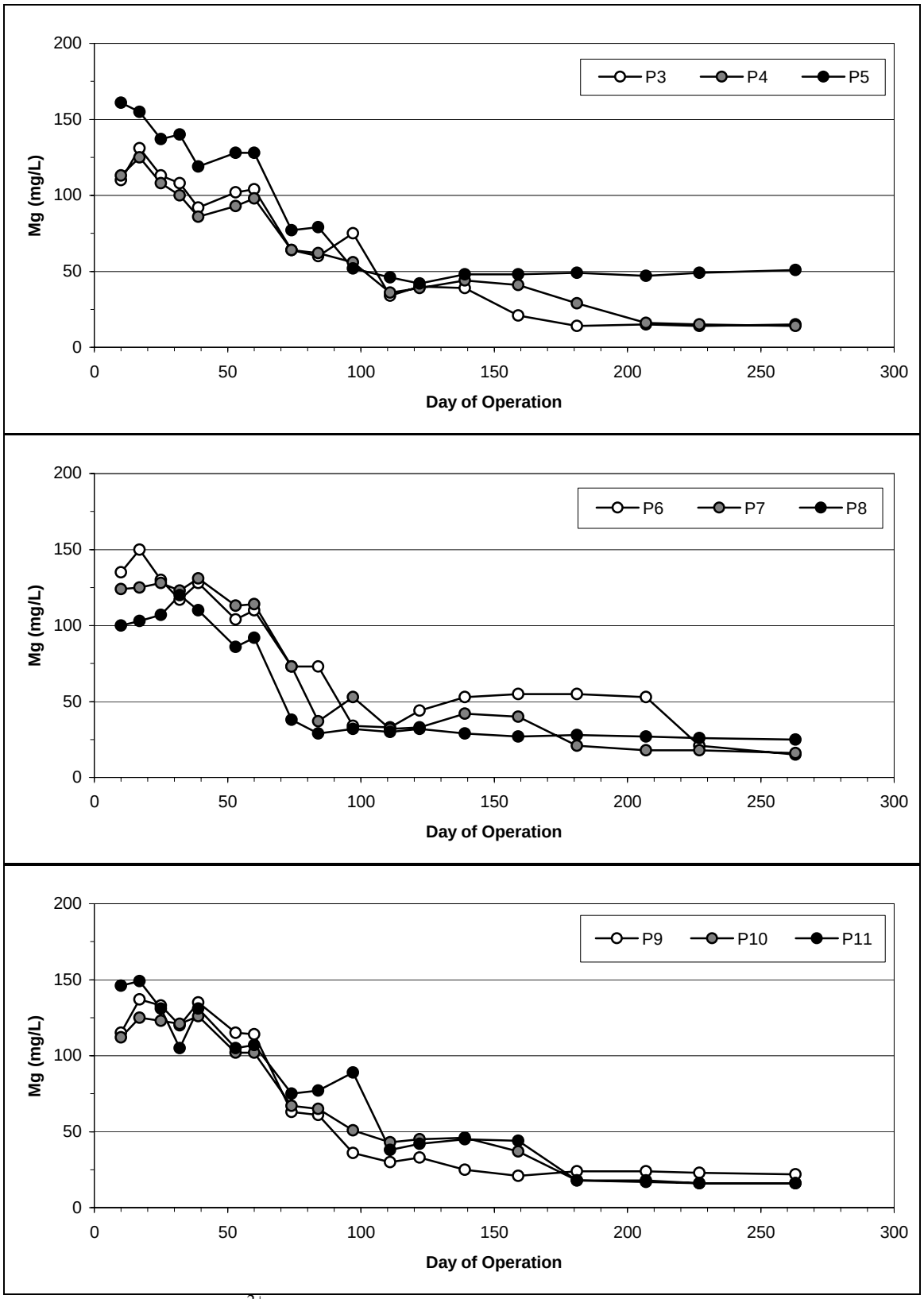

Figure B-8: Soluble Mg^{2+} in reactors P3-P11, divided by treatment.

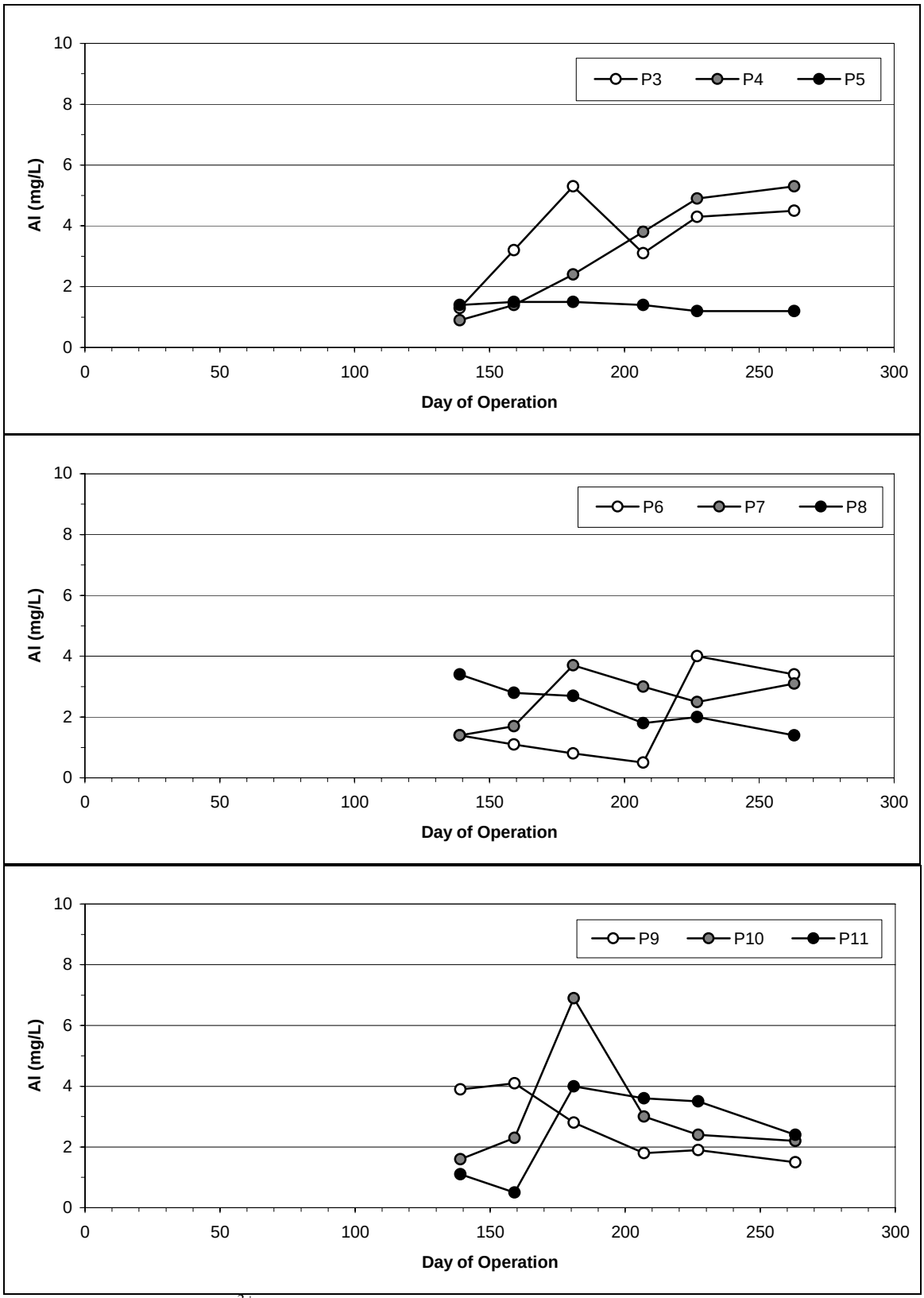

Figure B-9: Soluble Al^{3+} in reactors P3-P11, divided by treatment.

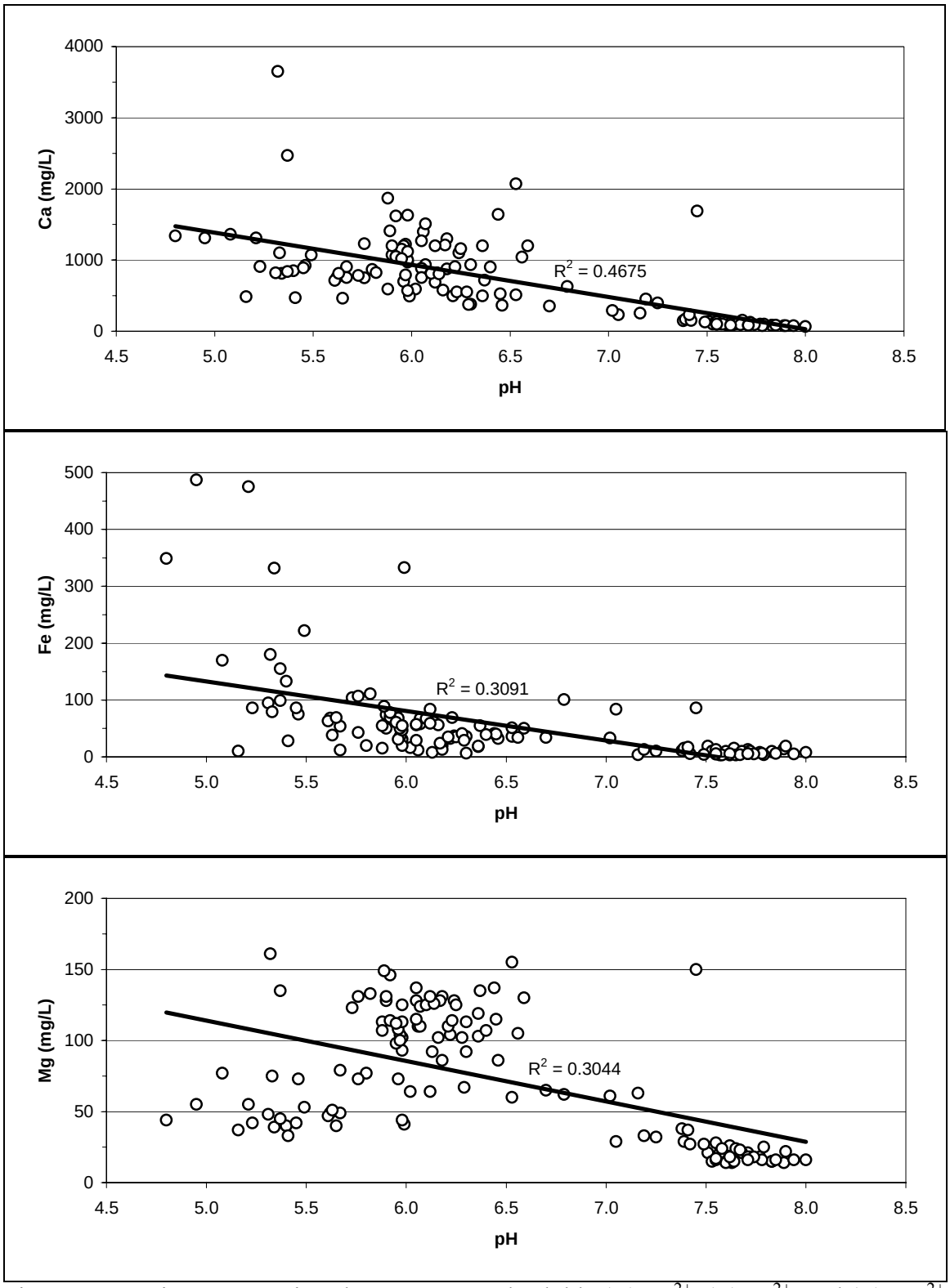

Figure B-10: Linear regressions between pH and soluble (A) Ca^{2+}, (B) Fe^{2+}, and (C) Mg^{2+} in reactors P3 to P11.

Table B-4**:** Results of alkalinity analyses performed on leachate collected from reactors P3-P11 on day 207 and filtered by 0.45 μm nylon. Alkalinity was measured by Standard Method 2320 (APHA, 1998).

Reactor	Alkalinity (mg $CaCO_3$/L)
P3	9618
P4	10084
P5	9307
P6	9283
P7	10551
P8	7130
P9	7800
P10	10934
P11	9977

Table B-5: Equilibrium modeling in MINTEQ of selected sampling dates in the P reactors. Sampling points were selected based on availability of Na^+ and K^+ data. Points with a wide range of pH values were input into the model to characterize both the acidic and methanogenic phases of refuse decomposition. Some runs do not include Al^{3+} as it was measured starting on day 139.

P3, day 60. Input pH: 5.97. Model-calculated charge difference: 96.7%.

Component (total dissolved)	Inputs (mg/L)	Outputs (mg/L)
Ca^{2+}	1220	1142.6
CO_3^{2-}	(0.5 atm CO_2)	1328.7
Fe^{2+}	36	15.0
K^+	3000	2999.9
Mg^{2+}	104	103.9
Na^+	5150	5152.2
NH_4^+	2275.7	2270.9
PO_4^{3-}	110.66	0.5

P4, day 181. Input pH: 7.05. Model-calculated charge difference: 39.9%.

Component (total dissolved)	Inputs (mg/L)	Outputs (mg/L)
Al^{3+}	2.4	0.0
Ca^{2+}	233	11.6
CO_3^{2-}	(0.5 atm CO_2)	6827.4
Fe^{2+}	84	0.1
K^+	696	696.0
Mg^{2+}	29	3.8
Na^+	4120	4121.8
NH_4^+	601.7	600.4
PO_4^{3-}	1.04	10.3

P5, day 74. Input pH: 5.8. Model-calculated charge difference: 96.2%.

Component (total dissolved)	Inputs (mg/L)	Outputs (mg/L)
Ca^{2+}	868	838.0
CO_3^{2-}	(0.5 atm CO_2)	1135.9
Fe^{2+}	20	20.0
K^+	1420	1420.0
Mg^{2+}	77	77.0
Na^+	2860	2861.2
NH_4^+	1388.6	1385.6
PO_4^{3-}	44.14	1.5

P6, day 122. Input pH: 4.8. Model-calculated charge difference: 98.9%.

Component (total dissolved)	Inputs (mg/L)	Outputs (mg/L)
Ca^{2+}	1340	1340.0
CO_3^{2-}	(0.5 atm CO_2)	806.3
Fe^{2+}	349	348.7
K^+	726	726.0
Mg^{2+}	44	44.0
Na^+	2450	2451.1
NH_4^+	464.1	463.1
PO_4^{3-}	185.25	185.3

P7, day 181. Input pH: 7.68. Model-calculated charge difference: 37.5%.

Component (total dissolved)	Inputs (mg/L)	Outputs (mg/L)
Al^{3+}	3.7	0.0
Ca^{2+}	154	1.6
CO_3^{2-}	(0.5 atm CO_2)	27427.8
Fe^{2+}	9.5	0.0
K^+	646	646.0
Mg^{2+}	21	0.5
Na^+	3950	3951.9
NH_4^+	488.6	487.5
PO_4^{3-}	13.21	149.4

P8, day 74. Input pH: 7.38. Model-calculated charge difference: 6.4%.

Component (total dissolved)	Inputs (mg/L)	Outputs (mg/L)
Ca^{2+}	148	3.7
CO_3^{2-}	(0.5 atm CO_2)	13639.2
Fe^{2+}	11	0.0
K^+	1220	1220.0
Mg^{2+}	38	1.1
Na^+	2140	2141.0
NH_4^+	1220.1	1217.5
PO_4^{3-}	31.71	33.5

P10, day 159. Input pH: 7.41. Model-calculated charge difference: 0.3%.

Component (total dissolved)	Inputs (mg/L)	Outputs (mg/L)
Al^{3+}	2.3	0.0
Ca^{2+}	231	3.4
CO_3^{2-}	(0.5 atm CO_2)	14887.2
Fe^{2+}	17	0.0
K^+	762	762.0
Mg^{2+}	37	1.1
Na^+	3970	3971.9
NH_4^+	811.3	809.6
PO_4^{3-}	8.11	46.1

P11, day 181. Input pH: 7.74. Model-calculated charge difference: 46.5%.

Component (total dissolved)	Inputs (mg/L)	Outputs (mg/L)
Al^{3+}	4	0.0
Ca^{2+}	93	1.4
CO_3^{2-}	(0.5 atm CO_2)	31393.2
Fe^{2+}	5.1	0.0
K^+	640	640.0
Mg^{2+}	18	0.4
Na^+	3740	3741.9
NH_4^+	414	413.1
PO_4^{3-}	22.77	190.3

Table B-6: MINTEQ outputs of P3 on day 159. The table presents equilibrium concentrations and activities of aqueous inorganic species.

Species	Concentration (moles/L)	Activity	Log activity
Al(OH)2+	4.74E-11	3.48E-11	-10.458
Al(OH)3 (aq)	8.65E-10	9.14E-10	-9.039
Al(OH)4-	2.16E-08	1.59E-08	-7.8
Al+3	2.09E-15	1.32E-16	-15.88
Al2(OH)2+4	1.34E-22	9.76E-25	-24.01
Al2(OH)2CO3+2	4.82E-16	1.41E-16	-15.851
Al2PO4+3	4.76E-21	2.99E-22	-21.524
Al3(OH)4+5	4.42E-28	2.03E-31	-30.692
AlHPO4+	1.02E-12	7.53E-13	-12.123
AlOH+2	2.74E-13	8.03E-14	-13.096
Ca(NH3)2+2	2.97E-12	8.69E-13	-12.061
Ca+2	2.58E-05	7.54E-06	-5.123
CaCO3 (aq)	5.61E-06	5.93E-06	-5.227
CaH2PO4+	1.37E-08	1.01E-08	-7.997

Species	Concentration (moles/L)	Activity	Log activity
CaHCO3+	3.09E-05	2.27E-05	-4.644
CaHPO4 (aq)	4.15E-07	4.39E-07	-6.358
CaNH3+2	1.57E-08	4.61E-09	-8.337
CaOH+	1.54E-10	1.13E-10	-9.945
CaPO4-	6.33E-08	4.65E-08	-7.332
CO3-2	1.30E-03	3.80E-04	-3.42
Fe(NH3)2+2	1.74E-11	5.09E-12	-11.293
Fe(NH3)3+2	3.21E-14	9.40E-15	-14.027
Fe(NH3)4+2	2.53E-17	7.40E-18	-17.131
Fe(OH)2 (aq)	9.35E-13	9.89E-13	-12.005
Fe(OH)3-	1.51E-15	1.11E-15	-14.953
Fe+2	2.10E-07	6.15E-08	-7.211
FeH2PO4+	2.71E-09	1.99E-09	-8.701
FeHCO3+	2.64E-07	1.94E-07	-6.713
FeHPO4 (aq)	3.07E-08	3.24E-08	-7.489
FeNH3+2	3.63E-09	1.06E-09	-8.974
FeOH+	2.25E-09	1.66E-09	-8.781
H+1	4.20E-08	3.09E-08	-7.51
H2CO3* (aq)	1.25E-02	1.33E-02	-1.878
H2PO4-	6.94E-05	5.10E-05	-4.292
H3PO4	2.31E-10	2.44E-10	-9.612
HCO3-	2.85E-01	2.10E-01	-0.678
HPO4-2	3.72E-04	1.09E-04	-3.963
K+1	1.62E-02	1.19E-02	-1.923
K2HPO4 (aq)	2.38E-07	2.52E-07	-6.599
K2PO4-	6.38E-11	4.69E-11	-10.329
KH2PO4 (aq)	1.46E-06	1.54E-06	-5.813
KHPO4-	1.63E-05	1.20E-05	-4.921
KOH (aq)	1.33E-08	1.40E-08	-7.852
KPO4-2	2.42E-09	7.07E-10	-9.151
Mg(NH3)2+2	1.28E-11	3.75E-12	-11.426
Mg+2	1.52E-05	4.46E-06	-5.351
Mg2CO3+2	1.00E-10	2.94E-11	-10.532
MgCO3 (aq)	1.55E-06	1.64E-06	-5.785
MgHCO3+	1.39E-05	1.02E-05	-4.991
MgHPO4 (aq)	3.39E-07	3.58E-07	-6.446
MgOH+	1.76E-09	1.29E-09	-8.889
MgPO4-	5.85E-10	4.30E-10	-9.366
Na+1	1.43E-01	1.05E-01	-0.979
Na2HPO4 (aq)	1.21E-05	1.28E-05	-4.892
Na2PO4-	1.05E-08	7.73E-09	-8.112
NaCO3-	7.73E-04	5.68E-04	-3.245
NaH2PO4 (aq)	1.28E-05	1.35E-05	-4.869
NaHCO3 (aq)	8.59E-03	9.08E-03	-2.042
NaHPO4-	2.22E-04	1.63E-04	-3.787
NaOH (aq)	8.91E-08	9.41E-08	-7.026
NaPO4-2	1.94E-08	5.66E-09	-8.247

Species	Concentration (moles/L)	Activity	Log activity
NH3 (aq)	7.15E-04	7.56E-04	-3.122
NH4+1	2.82E-02	2.07E-02	-1.684
OH-	9.20E-07	6.77E-07	-6.17
PO4-3	2.87E-08	1.81E-09	-8.743

Table B-7: MINTEQ outputs of P3 on day 159. The table presents equilibrated mass distributions of components among dissolved, sorbed, and precipitated phases.

Component	Total dissolved	% dissolved	Total sorbed	% sorbed	Total precipitated	% precipitated
Al+3	2.25E-08	100	0	0	0	0
Ca+2	6.28E-05	100	0	0	0	0
CO3-2	3.09E-01	100	0	0	0	0
Fe+2	5.13E-07	100	0	0	0	0
H+1	3.19E-01	100	0	0	0	0
K+1	1.63E-02	100	0	0	0	0
Mg+2	3.10E-05	100	0	0	0	0
Na+1	1.52E-01	100	0	0	0	0
NH4+1	2.89E-02	100	0	0	0	0
PO4-3	7.07E-04	100	0	0	0	0

Burnt Sugar Results

For the burnt sugar research, abiotic dissolution reactors ABS1 and ABS2 were 8-L polypropylene mason jars filled halfway with sand to which 1 L of sterile municipal solid waste leachate was added. The leachate was autoclaved using a 1-hour liquid sterilization cycle. After allowing the leachate to cool, 65 g/L sodium azide was dissolved in the leachate to prevent microbial regrowth. A 150 g layer of burnt sugar was poured onto the sand surface and the reactors were sealed. ABS1 and ABS2 were incubated at 35°C and 22°C, respectively, and their leachate was recirculated 4-5 times a week. The percent dissolution shown in Figure B-11 was calculated from the COD of the mass of BS added and the COD recovered in leachate.

Work was also conducted to determine the effect of BS addition on the pH of decomposing refuse. Solutions containing increasing concentrations of dissolved BS were mixed into well-decomposed refuse that had a neutral pH and a moisture content of about 60% to make a slurry. The pH was measured immediately after mixing. The results are summarized in Table B-8.

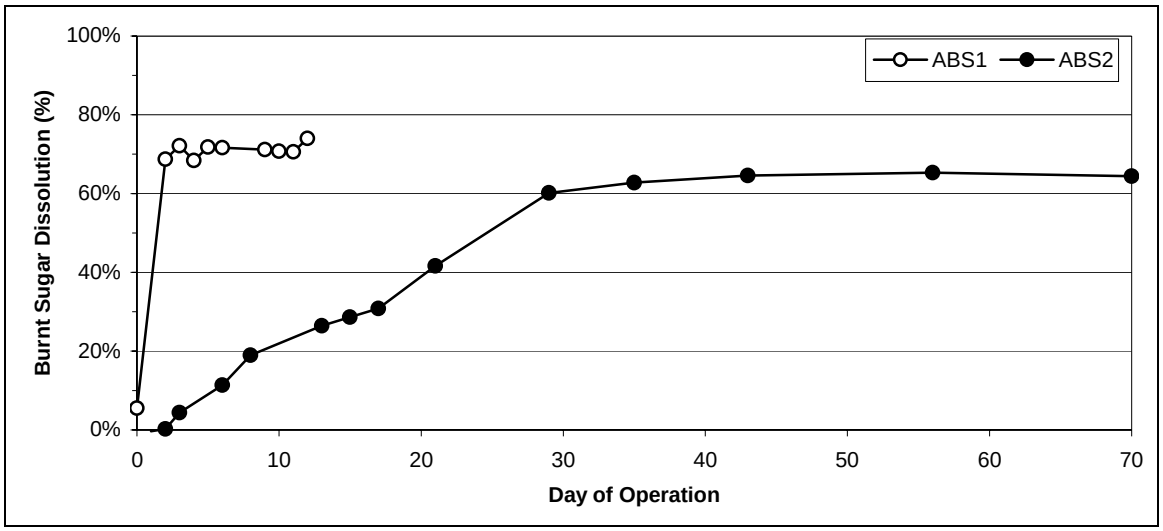

Figure B-11: Burnt sugar dissolution in abiotic reactors. Reactor ABS1 was incubated at 35°C and reactor ABS2 was incubated at 22°C. The y-axis is the percent of the added burnt sugar that was recovered in the leachate as calculated from the COD of the leachate and the COD of the mass of BS added.

Table B-8: Change in pH with burnt sugar additions.

Burnt Sugar Added / Weight of Refuse (g/dry kg)	pH
11.0	7.13
21.9	6.41
32.9	6.37
43.8	6.03
54.8	5.64
65.7	5.38
43.3	5.59
86.7	5.63
130.0	4.90
173.3	4.42

In preliminary work, VFAs were analyzed by the following technique. This technique is similar to that in the methods section, with one important difference: this method does not use the Dionex On-Guard H cartridges.

Acetic acid (ACS grade), was purchased from Sigma (USA), while propionic acid (99%) and n-butyric acid (99%) were purchased from Acros Organics (New Jersey, USA). Chemicals were used without further purification. Stock standard solutions of VFAs were made by transferring 0.5 g of pure chemical to a 10 mL volumetric flask and then filling it with methanol (HPLC grade, Fisher Scientific) to mark. Stock standard solutions of VFAs were stored at -20 ^{o}C. 5-mL leachate samples were acidified to pH 1-2 with concentrated HCl (certified grade, Fisher Scientific) and then filtered with glass microfiber GF/B syringe filters (25mm GD/X, Whatman). 2 mL filtrate was transferred to amber silanized 4-mL screw top vials (15mm x 45mm, Supelco, USA). 8 µL of 50 g/L 2-ethylbutyric acid was added as an internal standard. The vials were capped with phenolic caps and PTFE/silicone septa (11 mm). VFA standard solutions were made from diluting VFA standard stock solutions with DI water acidified to pH 2. Different concentrations of standard VFA solutions spiked with 8 µL of 50 g/L of 2-ethylbutyric acid were used to obtain the standard curve.

Solid phase microextraction (SPME) was used to extract VFAs from the acidified sample and standard solutions. Carbowax/divinylbenzene Stableflex fiber assemblies (70 µm, Supelco, PA.USA) were utilized to adsorb and concentrate VFAs from the solutions. The fiber was exposed to the headspace above the solution in the vials for 15 min at 25 ^{o}C. After adsorption, the fiber was injected directly into GC injector. The desorption time was 4 min. Fiber-adsorbed VFAs were separated by a HP G1800A GCD with DB-FFAP column (30m x 0.25mm x 0.85µm) and a mass spectrometry (Electron Ionization) detector. The temperature of the injector and detector were 220 ^{o}C and 280 ^{o}C, respectively. The initial temperature of the oven, 50 ^{o}C, was held for 0.5 min. The temperature was then increased to 100 ^{o}C at 20 ^{o}C/min. After holding at 100 ^{o}C for 5 min, the temperature was increased to 200 ^{o}C at 8 ^{o}C/min. The oven was held at 200 ^{o}C for 2 minutes. Carrier gas was He at flow rate 0.8 mL/min. EnviroQuant ChemStation G1701AA Version A.0300 software was used to for data collection and handling. Prior to any analysis, the mass spectrometry detector was autotuned with Perfluorotributylamine (PFTBA) tuning solution (Agilent, USA). Qualitative

identification of each VFA was based on the retention time and on mass spectrum match with NBS75K library. Selected Ion Monitoring (SIM) was used for quantification to lower the detection limit. The integrated abundance of the primary ion was used for quantitative analysis. Calibration curves with internal standard correction were used to calculate the concentrations of VFAs in the leachate samples.

Table B-9: Validation of VFA analysis method described above.

VFA	Standard conc. (ppm)	Calculated (ppm)	Recovery (%)	Standard conc. (ppm)	Calculated (ppm)	Recovery (%)
Acetic acid	2049.60	2155.50	105.17	4099.20	3894.62	95.01
Propionic acid	2101.76	2209.82	105.14	4203.52	4197.76	99.86
n-butyric acid	2000.00	1986.36	99.32	4000.00	3294.47	82.36

Table B-10: Spike tests for the VFA analysis method described above. All data were calculated from comparing the VFAs in samples after 100 ppm spiking to the VFAs in unspiked duplicate samples.

	ACH41	ACH42	NACH41	APOP1	APOP1	APOP1
	6/19/06	6/12/06	6/21/06	6/19/06	6/26/06	6/29/06
Acetic acid	75.2	97.1	-24.6	66.2	132.2	128.4
Propionic acid	67.5	99.8	-664.5	65.3	111.1	103.7
n-butyric acid	79.0	96.6	32.1	71.6	92.0	101.3

	APOP2	APOP2	APOP2	APOP2	ACH42	ACH42
	7/3/06	7/14/06	7/21/06	6/29/06	7/19/06	6/16/06
Acetic acid	102.8	80.8	78.6	91.8	108.2	116.4
Propionic acid	95.9	73.0	0.4	79.3	99.5	80.8
n-butyric acid	100.0	85.7	85.6	89.7	100.8	100.6

Table B-11: VFA Data for Reactor BS3.

Day of Operation	Method	Acetic Acid	Propanoic Acid	Butyric Acid
10.85	H cartridge	315.0	3306.1	40.0
12.83	No H cartridge	608.4	2358.6	66.5
14.71	H cartridge	220.4	<10.5	<10
17.75	No H cartridge	91.0	5.9	5.2
21.77	No H cartridge	30.7	105.4	1.5
24.83	No H cartridge	373.0	73.1	43.2
27.73	H cartridge	64.2	<10.5	<10
33.73	H cartridge	50.3	<10.5	<10
38.81	H cartridge	107.6	62.8	<40
42.67	No H cartridge	108.6	20.2	14.3
45.65	H cartridge	256.6	678.4	<40
47.85	H cartridge	34.6	<10.5	<10
49.79	No H cartridge	356.7	4280.1	48.2
52.75	H cartridge	239.6	<42	<40

Day of Operation	Method	Acetic Acid	Propanoic Acid	Butyric Acid
54.75	No H cartridge	25.2	41.4	<1
56.58	No H cartridge	172.9	3328.0	32.3
60.63	No H cartridge	51.3	8.8	3.3
62.68	No H cartridge	580.7	5896.7	120.9
67.69	No H cartridge	133.2	39.5	8.5
69.63	No H cartridge	611.6	3054.1	166.4
80.71	H cartridge	2336.5	>6305.3	4253.4
83.65	H cartridge	3842.8	5628.0	1197.7
87.59	H cartridge	1827.2	305.5	45.9
90.71	H cartridge	184.7	844.5	859.4
94.63	H cartridge	3517.1	>6305.3	3929.5
97.66	H cartridge	3679.1	>6305.3	3975.0
101.65	H cartridge	1827.7	2477.8	2799.4
104.83	H cartridge	2848.7	3263.1	3102.6
109.89	H cartridge	3937.8	3225.2	2238.4
112.67	H cartridge	3769.0	2359.9	774.7
116.73	H cartridge	3453.7	2777.4	3210.0
166.71	H cartridge	2649.0	2358.0	3519.4

Table B-12: VFA Data for Reactor BS4.

Day of Operation	Method	Acetic Acid	Propanoic Acid	Butyric Acid
10.85	No H cartridge	183.7	3309.1	6.6
14.71	No H cartridge	100.1	141.1	2.4
17.75	H cartridge	160.0	<42	<40
21.77	H cartridge	44.2	<10.5	<10
24.83	No H cartridge	383.6	226.6	56.4
27.73	H cartridge	23.6	<10.5	<10
31.88	No H cartridge	30.0	4.0	<1
33.73	No H cartridge	22.0	15.5	<1
38.81	H cartridge	65.1	<10.5	<10
42.67	H cartridge	51.1	<42	<40
47.85	No H cartridge	38.7	13.7	3.0
49.79	H cartridge	513.5	4838.9	45.2
52.75	H cartridge	201.6	234.3	<40
54.75	No H cartridge	64.5	40.5	7.1
56.58	No H cartridge	152.0	3657.8	24.8
60.63	No H cartridge	58.1	15.6	2.4
62.68	No H cartridge	525.1	5378.8	110.6
67.69	No H cartridge	153.7	114.2	9.9
69.63	No H cartridge	2188.9	8386.0	840.6
80.71	H cartridge	1258.0	5357.7	3370.8
83.65	H cartridge	3013.6	2483.1	175.2
87.59	H cartridge	695.1	68.7	<40
90.71	H cartridge	901.4	>6305.3	4271.2
94.63	H cartridge	1306.2	5085.6	2866.6
97.66	H cartridge	2703.2	5300.1	1135.6

Day of Operation	Method	Acetic Acid	Propanoic Acid	Butyric Acid
101.65	H cartridge	3434.9	2408.1	88.8
104.83	H cartridge	2495.6	<42	<40
109.89	H cartridge	278.4	<42	<40
112.67	H cartridge	176.7	<42	<40
116.73	H cartridge	872.7	2619.3	2963.8
166.71	H cartridge	1241.4	2121.7	3354.3

Table B-13: Methane recovery calculations in A) BS3 and B) BS4.

Reactors	Refuse	Sugar Addition (g/dry kg refuse)	Avg. Measured Cumulative CH4 (mL/dry g)	Measured CH4 (L)
BS1 and BS2 Averages (control)	818.4	0	84.2	68.9
BS3 (BS solution addition)	824.3	921.3	253.5	208.9

Measured CH_4 from Sugar Addition (L)	140.1
Theoretical CH_4 from COD Accumulation (L)	95.1
Theorectical CH_4 from Leachate Samples (L)	8.3
Theoretical CH_4 from Sugar Addition (L)	326.9
Methane Recovery	**74.5%**

Reactors	Refuse	Sugar Addition (g/dry kg refuse)	Avg. Measured Cumulative CH4 (mL/dry g)	Measured CH4 (L)
BS1 and BS2 Averages (control)	818.4	0	84.2	68.9
BS4 (BS solution addition)	822.7	923.1	272.1	223.8

Measured CH_4 from Sugar Addition (L)	155.0
Theoretical CH_4 from COD Accumulation (L)	80.0
Theorectical CH_4 from Leachate Samples (L)	6.7
Theoretical CH_4 from Sugar Addition (L)	326.9
Methane Recovery	**73.9%**

The methane recovery was calculated as the percent of the expected methane and methane potential that could be accounted for divided by the methane potential of the added BS. For example, in BS3, the measured methane attributable to the BS addition was 140.1 L while the methane potential was 95.1+8.3L for a total methane recovered of 243.5L. This represents 74.5% of the amount of methane potential added as BS. In BS4, more methane was produced less COD accumulated, which gave a similar methane recovery percentage as BS3.